INVESTIGATION OF EDGE CRACKING PROPENSITY IN COLD-ROLLED COMMERCIAL ALUMINIUM ALLOY 8011 UNDER MIXED OIL LUBRICATION CONDITION

BY

HASSAN ONIMISI YAKUBU

DEPARTMENT OF METALLURGICAL AND MATERIALS ENGINEERING

AHMADU BELLO UNIVERSITY, ZARIA

NIGERIA.

JULY, 2014

INVESTIGATION OF EDGE CRACKING PROPENSITY IN COLD-ROLLED COMMERCIAL ALUMINIUM ALLOY 8011 UNDER MIXED OIL LUBRICATION CONDITION

By

Hassan Onimisi YAKUBU, B. Eng (Met.), A. B. U. 2006

M.Sc/ENG/ 12822/2010-2011

A THESIS SUBMITTED TO THE SCHOOL OF POSTGRADUATE STUDIES, AHMADU BELLO UNIVERSITY, ZARIA.

IN PARTIAL FULFILLMENT OF THE REQUIREMENTS FOR THE AWARD OF A

MASTER DEGREE IN METALLURGICAL AND MATERIALS ENGINEERING

DEPARTMENT OF METALLURGICAL AND MATERIALS ENGINEERING,

FACULTY OF ENGINEERING

AHMADU BELLO UNIVERSITY, ZARIA

NIGERIA.

JULY, 2014

DECLARATION

I declare that the work in this thesis entitled Investigation of Edge Cracking Propensity in Cold-Rolled Commercial Aluminium Alloy 8011 under mixed oil Lubrication Condition has been carried out by me in the Department of Metallurgical and Materials Engineering, Ahmadu Bello University, Zaria. The information derived from the literature has been duly acknowledged in the text and a list of references provided. No part of this thesis was previously presented for another degree or diploma at this or any other institution.

Hassan Onimisi YAKUBU ……..…… ……...…….

Name of Student Signature Date

CERTIFICATION

This thesis entitled Investigation of Edge Cracking Propensity in Cold-Rolled Commercial Aluminium Alloy 8011 under mixed Oil Lubrication Condition by Hassan Onimisi YAKUBU meets the regulations governing the award of the degree of Master in Metallurgical and Materials Engineering of the Ahmadu Bello University, and is approved for its contribution to knowledge and literacy presentation.

Prof. A. K. Oyinlola	…….	……
Chairman, Supervisory Committee	Signature	Date
Dr. G. B. Nyior	……	……
Member, Supervisory Committee	Signature	Date
Prof. S. A. Yaro	…….	……...
Head of Department	Signature	Date
Prof. A. A. Joshua	……	……
Dean, School of Postgraduate Studies	Signature	Date

DEDICATION

This thesis is dedicated to:

- The Almighty Allah, the Most Beneficent and the Most Merciful.
- The lingering memory of my dearly beloved father and sister, Mallam Yakubu Okara Onimisi and Yakubu Fatimoh respectively. Find solace in the bosom of the Lord (Amin).

ACKNOWLEDGEMENTS

First and foremost, my gratitude goes to the Almighty Allah, the Sustainer of life who had made the completion of this thesis a reality.

I would like to thank my supervisors, Prof. A. K. Oyinlola and Dr G. B. Nyior for their continued encouragement and selfless contribution to the completion of this work. My appreciation also goes to the Lecturers of the Department of Metallurgical and Materials Engineering who might have in one way or the other contributed to the success of this thesis. I also acknowledge the effort of Technologists/Technicians in the Departments of Metallurgical and Materials Engineering, and Mechanical Engineering of Ahmadu Bello University, Zaria for their contribution in the practical aspect of the work.

The assistance rendered by Tower Aluminium Rolling Mills, Ota Ogun State in providing useful information, materials and equipment for this research work is greatly appreciated. God may continue to support and bless the company as a leading producer of rolled aluminium products in Nigeria. Special appreciation must be given to the Engineers at Tower Aluminium Rolling Mills for the kind assistance rendered during the practical aspect of the work.

My dear wife, Sikirat Oyiza Yakubu is the person who should be given special attention. Her encouragement, patience, perseverance and support are highly appreciated. Your effort is inestimable – Thanks a lot, dear!!! I also acknowledge my kids, Abdullateef and Fussilat who always find it difficult to cope during my absence. God bless you all.

My appreciation goes to my parents for their massive support and understanding during my study. I also acknowledge my friends who have contributed to the success of this project. God reward you all abundantly.

ABSTRACT

The effect of iron content on edge cracking tendency in cold-rolled commercial aluminium alloy 8011 under a mixed coconut/diesel oil (factory formulated oil) lubrication condition and under neem seed oil as an alternative has been investigated. Three different aluminium alloy plates each containing 0.708%Fe, 0.909%Fe and 0.931%Fe were produced by chill casting method. Seven samples each of dimension 240mm x 140mm x 7mm were cast per alloy. As-received commercial aluminium alloy 8011 of 0.857%Fe was cut into seven samples of the same geometry. Experimentation involved cold reduction in thickness by rolling at various degrees of deformation, followed by testing of mechanical properties and qualitative metallographic analysis. Performance evaluation of mixed coconut/diesel oil and neem seed oil lubricants in friction reduction of cold-rolled commercial AA 8011 and proportion of mixture of coconut and diesel oil that will give the highest percentage deformation were also conducted by plane strain compression test. From the results obtained, it was observed that aluminium alloy 8011 generally exhibited softening characteristics as shown by its maximum ultimate tensile strength of 176.45MPa at 60% reduction in thickness and on reaching the peak hardness values, all samples displayed decrease hardness for given levels of percent reduction in thickness. It was also observed that for up to a maximum of 0.931%Fe, AA 8011 could be cold-rolled to a maximum of 60% reduction in thickness without any evidence of edge cracking. Alloys with 0.909%Fe and 0.931%Fe, edge cracked at 70% and 80% reductions in thickness and the other alloys showed no edge cracking for the whole percentage deformations investigated. Furthermore, samples of AA 8011 containing more than 0.9%Fe revealed higher tensile strength when cold-rolled to 80% reduction in thickness. The results of plane strain compression test showed that at any specific load, neem seed oil provided better lubrication; about 106% reduction in thickness better than

mixed coconut/diesel oil at100kN load. The mixture of locally sourced coconut and diesel oil in different proportions performed best in friction reduction at the ratio of 30% coconut oil and 70% diesel.

TABLE OF CONTENTS

Title Page……..……i

Declaration……..…….ii

Certification…….…….....iii

Dedication……..…….iv

Acknowledgements……..……v

Abstract…….....…vi

Table of Contents……..…….viii

List of Figures…….……...xiii

List of Tables…….……xv

List of Plates……..xvi

1.0 INTRODUCTION…….……..……...1

1.1 Statement of the Research Problem……..…….……...2

1.2 Justification……..3

1.3 Aim and Objectives……..……..……...……...4

1.4 Scope of the Work ……..…….5

1.5 Contribution to Knowledge……...……..5

2.0 LITERATURE REVIEW……..……..……...…7

2.1 Introduction……..7

2.2 Metal Rolling Process……..……7

2.2.1 Hot-rolling……...8

2.2.2 Cold-rolling……9

2.2.3 Mechanics of Rolling Process…….……9

2.2.4 Pressure Distribution along the Arc of Contact and Roll Bite Condition…….…….....12

2.3 Problems and Defects in Rolled Products……13

2.3.1 Edge Cracking……...14

2.3.2 Causes of Edge Cracking……..15

2.4 Friction and Lubrication in Metal Working Processes……..…18

2.4.1 Mode of Lubrication in Cold Rolling……..…….19

2.4.2 Evaluation of Lubricants in Cold Rolling by Plane Strain Compression Test…….....20

2.4.3 Chemical Analysis of Lubricating Oils…….....22

2.5 Effect of Iron on Aluminium Alloys…….....23

2.5.1 Effect of Iron on the Mechanical and Structural Properties of Aluminium Alloys……..…25

3.0 MATERIALS, EQUIPMENT AND GENERAL EXPERIMENTAL PROCEDURES..30

3.1 Introduction……30

3.2 Materials……30

3.2.1 Commercial Aluminium Alloy 8011……30

3.2.2 Mixed Coconut/diesel and Neem Seed Oil……...……....31

3.3 Equipment……..31

3.4 Experimental Procedures…….....32

3.4.1 Casting of Alloys……..32

3.4.2 Cold Rolling Experiment…….....33

3.4.3 Tensile Strength Test…….……...34

3.4.4 Hardness Test……....35

3.4.5 Impact Strength Test…….…....35

3.4.6 Metallographic Examination……..…....36

3.4.7 Chemical Analysis of the Investigated Oils…….……..…...36

3.4.8 Plane Strain Compression Test……...……..37

4.0 EXPERIMENTAL RESULTS…….……39

4.1 Introduction……39

4.2 Evaluated Mechanical Properties…….....39

4.3 Microstructural Examination of AA 8011…….....40

4.4 Chemical Analysis of the Investigated Oils……..……...41

4.5 Lubrication Potential of the Investigated Oils in Cold Rolling of AA 8011 by Plane Strain Compression Test……..…….....42

5.0 DISCUSSION OF THE EXPERIMENTAL RESULTS……..…….....44

5.1 Introduction……44

5.2 Edge Cracking Characteristics of Aluminium Alloy 8011 of Varying Iron Contents Cold-rolled to Various Reductions in Thickness…….....44

5.3 Effect of Iron Content on Tensile Properties of Cold-rolled Samples of AA 8011……...…….....……..……..45

5.4 Effect of Iron Content on Ultimate Tensile Strength of Cold-rolled Samples of AA 8011……..47

5.5 Effect of Iron Content on Ductility of the Cold-rolled Samples of AA 8011……....49

5.6 Effect of Iron Content on Hardness Properties of Cold-rolled Samples of AA 8011……...……51

5.7 Effect of Iron Content on Impact Strength of Cold-rolled Samples of AA 8011……..……..…….52

5.8 Effect of Iron Content on Microstructures of Cold-rolled Samples of AA 8011……..…….53

5.9 Evaluation of Lubricants in Cold Rolling Process ……..54

5.10 Evaluation of Proportions of Mixture of Coconut and Diesel Oils in Cold Rolling Process ……..……..56

6.0 SUMMARY, CONCLUSION AND RECOMMENDATIONS…..……58

6.1 Summary…….……58

6.2 Conclusion……...……...58

6.3 Recommendations……..……59

REFERENCES…….61

APPENDICES……..……68

Appendix A……..…….68

Appendix B……...72

Appendix C……...……76

LIST OF FIGURES

Figure 1.1 Edge crack on cold-rolled aluminium alloy ……..……..…….1

Figure 2.1: Schematic drawing of rolling process (flat rolling)……..….8

Figure 2.2: Schematic drawing of flat rolling without top roll……9

Figure 2.3: Forces acting during rolling……..……9

Figure 2.4: Distribution of roll pressure along the length of contact……..…...12

Figure 2.5: Component of forces in rolling process……..……12

Figure 2.6: Schematic illustration of typical defects in flat rolling……...14

Figure 2.7: Possible elastic deformation mode of work rolls during cold rolling…….17

Figure 2.8: A schematic diagram of the plane strain compression test…….....22

Figure 2.9: Ternary Al-Si-Fe phase diagram…….28

Figure 3.1: A photograph of the flat mill showing various mechanisms……..…….34

Figure 5.1: Chart of ultimate tensile strength against percent cold-rolled reduction in thickness……...……..47

Figure 5.2: Graph of ductility against percent cold-rolled reductions in thickness……...…49

Figure 5.3: Graph of hardness values against cold-rolled reduction in thickness for the investigated alloy samples of AA 8011……..…51

Figure 5.4: Graph of impact strength against cold-rolled percent reduction in thickness……..……..52

Figure 5.5: Reduction capacity of the investigated oils under plane strain compression test……..……54

Figure 5.6: Reduction capacity of the locally sourced coconut oil mixed with diesel in various proportions under plane strain compression test…….....56

Figure B1: Stress-strain curves of as-received and as-cast samples……..…...72

Figure B2: Stress-strain curves of samples cold-rolled to 30% reduction in thickness…….....72

Figure B3: Stress-strain curves of samples cold-rolled to 40% reduction in thickness…….....73

Figure B4: Stress-strain curves of samples cold-rolled to 50% reduction in thickness…..……..73

Figure B5: Stress-strain curves of samples cold-rolled to 60% reduction in thickness…….....74

Figure B6: Stress-strain curves of samples cold-rolled to 70% reduction in thickness…..……...74

Figure B7: Stress-strain curves of samples cold-rolled to 80% reduction in thickness…….....75

LIST OF TABLES

Table 3.1: Chemical composition of commercial aluminium alloy 8011……..……30

Table 3.2: Chemical composition of as-received commercial aluminium alloy 8011……..…31

Table 3.3: Chemical compositions of as-cast and as-received aluminum alloy 8011……..….32

Table 3.4: Investigated rolling schedule……....33

Table 4.1: Mechanical properties of Aluminium Alloy 8011…….....……40

Table 4.2: Fatty acids composition of the investigated oils……..…….41

Table 4.3: Saponification value and free fatty acid of the investigated oils……..……41

Table 4.4: Performance evaluation of mixed coconut/diesel and neem seed oils in cold rolling of the as-received AA 8011 assessed by plane strain compression…….....42

Table 4.5: Performance evaluation of mixed oil lubrication in various proportions (coconut and diesel oil) in cold rolling of the as-received AA 8011 assessed by plane strain compression test……..43

LIST OF PLATES

Plate A1: Aluminium Alloy 8011 cold-rolled to 30% reduction in thickness……..…….68

Plate A2: Aluminium Alloy 8011 cold-rolled to 40% reduction in thickness……..…….69

Plate A3: Aluminium Alloy 8011 cold-rolled to 50% reduction in thickness……..….69

Plate A4: Aluminium Alloy 8011 cold-rolled to 60% reduction in thickness……..….70

Plate A5: Aluminium Alloy 8011 cold-rolled to 70% reduction in thickness……..….70

Plate A6: Aluminium Alloy 8011 cold-rolled to 80% reduction in thickness……..….71

Plate C1: Optical micrographs of as- received and as-cast samples AA 8011……..…76

Plate C2: Optical micrographs of samples AA8011cold-rolled at 80% reduction in thickness.…….……..77

CHAPTER ONE

1.0 INTRODUCTION

The rolling of slab or sheet metals is probably one of the most advanced techniques among metal working processes due to its high productivity and close control of the final products. The majority of the basic processes were invented during the second half of the 19th century; since then, thousands of patents have been added which have improved the efficiency of the process or some part of the machinery used in the performance of the rolling operation (Schey, 1966).

Cold rolling process is one of the industrial practices employed in the manufacturing of plate, sheet, strip and foil products of aluminium and its alloys. In spite of this very intensive activity, the problem of edge cracking which accompanies rolling process has not been completely resolved. Acceptable ways and means of preventing this defect is a challenge to commercial aluminium rolling operators. Cracking along the edge of a cold-rolled strip as shown in Figure 1.1 is a defect which affects the quality of the product.



Figure 1.1 Edge crack on cold-rolled aluminium alloy (Haibo, 2011)

Edge cracking is a commonly observed phenomenon in the cold rolling process which costs the production industry millions of dollars each year (Haibo, 2011). Subsequent edge trimming of the cracked material becomes necessary and this leads to significant loss in productivity. In a typical aluminium plant, only about 50% of the original material makes it through to the final product form (Ghosh *et al.,* 2004). The rest of the materials are lost in various stages of the production processes and are returned to the melting furnace. Edge trimming represents a large proportion of this loss.

In aluminium industries, edge cracking may penetrate to a depth such that subsequent utilization of the rolled product to produce finished article is not possible and the material has to be re-melted. This accounts for zero efficiency despite the cost of fuel, electricity and man-power involved in the melting process (Haibo, 2011).

The phenomenon of ductile failure such as edge cracking in cold rolling of metals and alloys is complex. It depends on the macroscopic factors such as roll geometry, rolling speed, reduction ratios or pass schedule, lubrications or friction, alloys and temper, and mechanical properties as well as microscopic factors such as microstructure and surface micro-topography (Ghosh *et al.,* 2004). Some of these parameters can be varied to obtain the best mechanical properties of the rolled products.

1.1 Statement of the Research Problem

Commercial aluminium alloy 8011 is mainly an Al-Fe-Si alloy, which has a wide variety of end applications owing to the fact that it is possible to control the microstructural composition of the alloy by means of specific thermal and mechanical treatments (Xing *et al.,* 2001).

The Tower Aluminium Rolling Mills, Ota Ogun State, which is a leading producer of aluminium rolled products in Nigeria, is experiencing the difficulty of reducing to an acceptable level, the edge cracking defect, which often accompanies rolling process, both in hot- and cold-rolling of commercial AA 8011. The company produces semi-finish rolled products which are subsequently rolled to finish products such as roofing sheets, cooking pots and other kitchen utensils.

The company formerly rolls commercial AA 1200 containing a minimum of 99% pure aluminium where edge cracking defect was found to have been reduced to an acceptable level in the rolling of the alloy. Its low strength coupled with high cost of aluminium ingots led to the shift to an alternative AA 8011.

This work seeks to investigate the possibility of reducing edge cracking defect in cold-rolled commercial aluminium alloy 8011 to an acceptable level by varying the iron content as well reducing rolling frictional effect using various lubricants. The optimum iron content and the most effective lubricating oil which reduces edge cracking tendency will be established.

1.2 Justification

Edge cracking- a defect associated with limited ductility of material and commonly encountered in the rolling of commercial alloys- has been a difficult problem facing rolling mill industries. In many rolled materials, subsequent edge trimming of the cracked edge becomes necessary and this leads to significant economic losses.

Prevention of edge cracking in rolling of commercial alloys by means of edge restraints proposed by Schey (1966) is inadequate for predesigned rolling mills for specific

operation; also the cold-work-anneal cycle is not a feasible approach in commercial rolling operation.

Composition adjustment of the alloying elements which are deleterious to the ductility of the commercial alloy and the most effective lubricant that will enhance friction reduction become attractive possibilities for the prevention of edge cracking. If optimum iron content and the oil with the best lubrication property in rolling of AA 8011 that will give the best mechanical properties (ductility in particular) with acceptable level of edge cracking are established, this may solve the problem of edge cracking facing commercial aluminium rolling mills industries and this will enhance their productivity.

1.3 Aim and Objectives

i. To investigate edge cracking defect in cold rolling of aluminium alloy 8011 of varying iron contents under mixed coconut/diesel oil lubricant.
ii. To establish the maximum iron content that will give the best mechanical properties with reduction in edge cracking tendency in rolling operation of commercial aluminium alloy 8011.
iii. To determine the effect of mechanical working operation (rolling) on tensile strength, impact strength and hardness of the aluminium alloys with the aim of evaluating the mechanical properties of the alloys.
iv. To compare the effectiveness of neem seed oil with the commercially used mixed coconut/diesel oil in reducing edge cracking defect in cold-rolled commercial AA 8011.

v. To provide background information for further research work on minimizing edge cracking in rolling of commercial aluminium alloys.

1.4 Scope of the Work

The scope cover;

i. Casting of the aluminium alloys of varying iron content within the rages of AA 8011 by chill casting method.
ii. Annealing of the cast alloys.
iii. Mechanical working operation (rolling) and evaluation of the mechanical properties of the alloys.
iv. Composition and microstructural examinations of the cast alloys.
v. Comparison of lubricity potentials of mixed coconut/diesel oil as lubricant and neem seed oil as substitute in cold rolling of AA 8011 by plain strain compression test.
vi. Determination of proportion of mixture of coconut oil and diesel that will give the highest percentage deformation in cold rolling of AA 8011 by plain strain compression rest.

1.5 Contribution to Knowledge

Many researchers have carried out work on the possibility of improving the mechanical properties, particularly the ductility of commercial alloys in rolling process, with the aim of eliminating edge cracking by compositional adjustment and other means.

This research work has established the following

i. The optimum iron content which gave the best mechanical properties with tolerable edge cracking in rolling of commercial aluminium alloy 8011.

ii. The suitability of neem seed oil as lubricant for friction reduction in cold rolling operation as an effective alternative for friction reduction in the event of it being a contributive parameter to edge cracking defect observed in the cold rolling process.

iii. The optimum ratio of mixture of coconut oil and diesel that will give the highest percentage deformation in cold-rolled commercial AA 8011.

CHAPTER TWO

2.0 LITERATURE REVIEW

2.1 Introduction

In this chapter a detailed analysis of selected aspect of extensive literatures concerning cold rolling principle and effects of iron in aluminium alloys will be presented in order to assess the theory of two possible causes that may contribute to the formation of edge cracking defect. This chapter begins with brief description of the metal rolling process followed by problems and defects in rolled products and friction and lubrication in metal working processes. The effect of iron on aluminium alloys in forming interdendritic phase particles which greatly influence the mechanical and structural properties of the aluminium alloys have also been studied.

2.2 Metal Rolling Process

Rolling is a process of plastically deforming metal in which its thickness is reduced by compressive forces exerted by two opposing rolls. It is the most widely used metalworking process because of its high production rate and close control of final products. As a result of the frictional action of the rolls, the metal is drawn into the rolls and squeezed to reduce its thickness. The schematic diagram showing rolling process is given in Figure 2.1

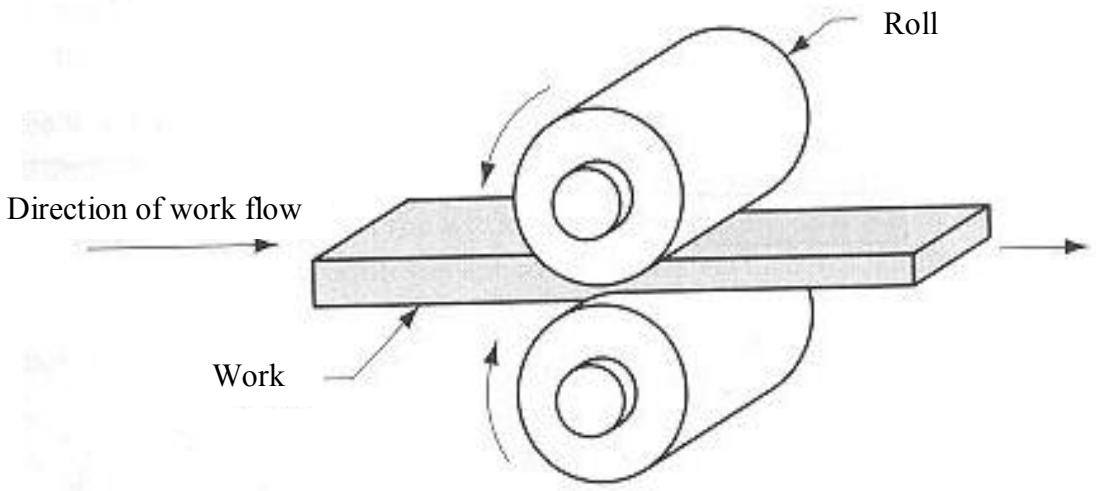


Figure 2.1: Schematic diagram of flat rolling process (Naser and Tom, 2008)

Rolling of metals can be performed hot (hot-rolling) or cold (cold-rolling).

2.2.1 Hot-rolling

Rolling of metal above the recrystallization temperature, but below the melting point is called hot rolling. The breakdown of ingot into bloom, billet or slab is usually carried out by hot rolling. The objective of this operation is to produced semi-finished product for subsequent production of bar, plate or sheet. The initial breakdown passes often involve only a small reduction. There is an appreciable spreading of the ingot width in hot rolling. Spreading is expected because of the volume constancy in plastic deformation. Since the material is compressed in the thickness direction, both the length and width will increase provided that the material is not constrained in the width direction (Dieter, 1988).

Spreading is more pronounced with low width-to-thickness ratios and low coefficients of friction, since there is small resistance to flow in the width direction. Large amount of deformation is possible in hot rolling and at the same time the hot rolled material is of reduced residual stresses, and has isotropic properties. The disadvantage of hot-rolling is

that it does not have close dimensional control, and surface has a characteristic oxide scale (Dieter, 1988).

2.2.2 Cold-rolling

Rolling of metals at such a temperature and strain rate that recrystallization does not occur is called cold rolling. Cold-rolling process is used to produce a sheet or strip with good surface finish and close dimensional control. Cold rolling results in loss of ductility and increase of strength and hardness because of the strain hardening which usually accompanies the process. Cold rolled sheet can be produced in various conditions such as skin-rolled, quarter-rolled, half hard and full hard depending on how much cold work has been performed (Oginsky, 2011).

2.2.3 Mechanics of Rolling Process

Figure 2.2 illustrates the schematic drawing of flat rolling process and Figure 2.3 illustrates a number of relevant relationships between the geometry of the rolls and the force involved in deforming metal by rolling.

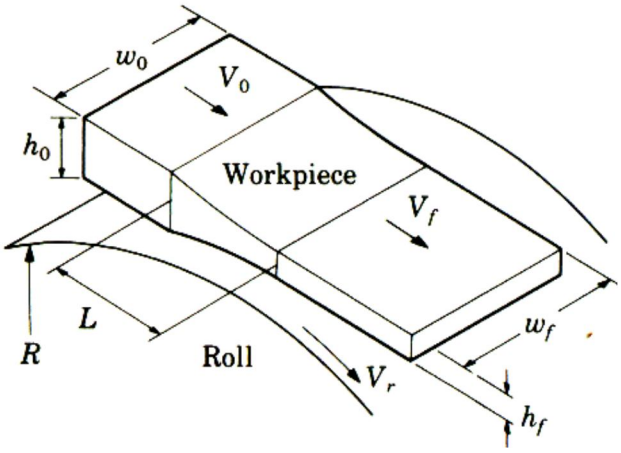


Figure 2.2: Schematic drawing of flat rolling without top roll (Oginsky, 2011).

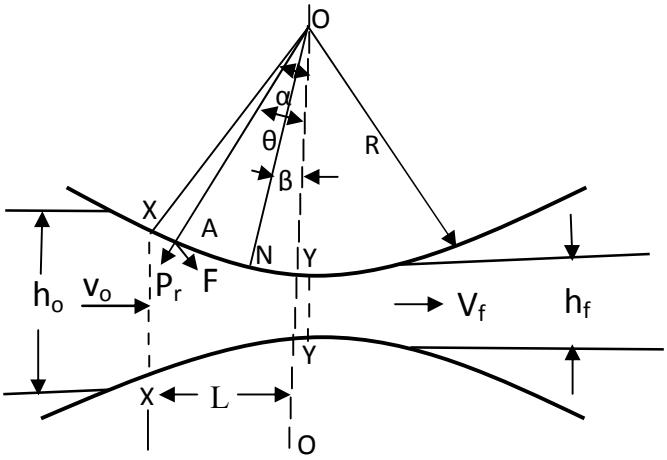


Figure 2.3: Forces acting during rolling (Dieter, 1988).

A workpiece of thickness h_o enters the rolls at the entrance plane XX with a velocity V_o and passes through the rolls gap and leaves through the exit plane YY with a reduced thickness h_f. Since rolling is assumed to be plane strain condition, no increase in width results, so that the vertical compression of the metal is translated into an elongation in the rolling direction. Since equal volume of metal must pass a given point per unit time, it implies that; (Dieter, 1988)

$$whv = wh_ov_o = wh_fv_f \tag{2.1}$$

where w = width of workpiece

v = velocity at any thickness h intermediate between h_o and h_f.

Given that $w_o = w_f$, then $h_ov_o = h_fv_f$.

This implies that $$\frac{V_0}{V_f} = \frac{h_f}{h_0} \tag{2.2}$$

When $h_o > h_f$, we then have $v_o < v_f$

Since the volume is constant, the velocity of the workpiece must steadily increase from entrance to exit such that a vertical element in the workpiece remains undistorted. At the exit of the roll gap, the workpiece moves with velocity V_f and because V_r is constant along the roll gap, sliding occurs between the roll and the strip. At any point along the surface of contact, such as point A in Figure 2.3, two forces act on the workpiece. These are radial force P_r and tangential friction force F. At a certain point along the arc of contact, strip velocity and roll velocity are the same. This is known as neutral point, or no slip point (Dieter, 1988).

To the left of the neutral point, roll moves faster than the strip, and the frictional force acts in the direction shown in Figure 2.3 so as to draw the strip into the rolls. To the right of the neutral point, the strip moves faster than the roll and the direction of the frictional force is reversed so that it acts to oppose the delivery of the strip from the rolls.

The vertical component of radial force, P_r is known as the rolling load, P. The specific roll pressure, ρ is the rolling load divided by the contact area. The contact area between the metal and the rolls is equal to the product of the width of the sheet, w and the projected length of the arc of contact, L (Dieter, 1988).

$$L = [R(h_0 - h_f) - \frac{(h_{0-h_f})^2}{4}]^{1/2} \approx [R(h_0 - h_f)]^{1/2}$$

$$L \approx \sqrt{R\Delta h} \qquad (2.3)$$

Therefore, the specific roll pressure is given by $\rho = \frac{P}{wL}$ (2.4)

2.2.4 Pressure Distribution along the Arc of Contact and Roll Bite Condition

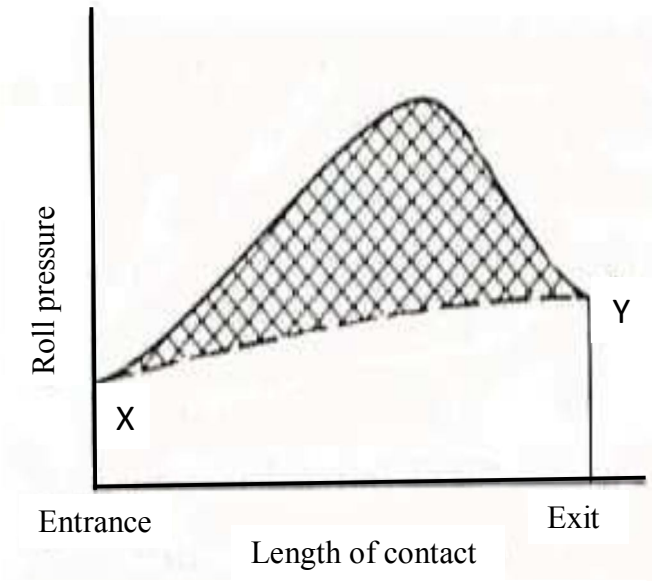


Figure 2.4: Distribution of roll pressure along the length of contact (Dieter, 1988).

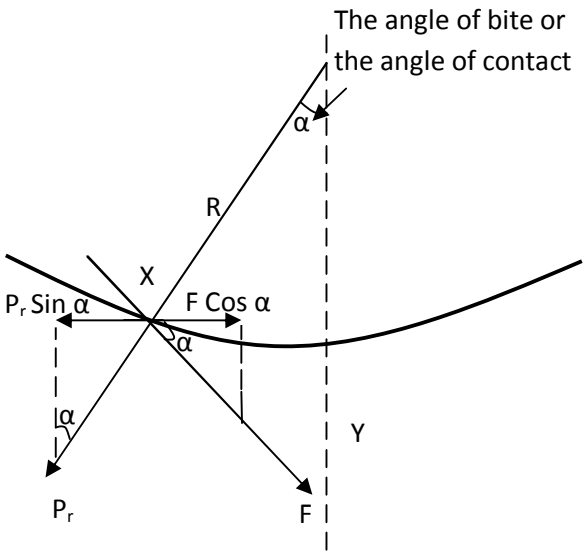


Figure 2.5: Component of forces in rolling process (Oginsky, 2011).

The distribution of roll pressure along the arc of contact shows that the pressure rises to a maximum at the neutral point and then falls off. The pressure distribution does not come to a sharp peak at the neutral point, which indicates that the neutral point is not really a line on the roll surface but an area (Dieter, 1988).

The area under the curve is proportional to the rolling load. The shaded area represents the force required to overcome frictional forces between the roll and the sheet. The area under the dashed line XY represents the force required to deform the metal in plane homogeneous compression.

From Figure 2.5, for the workpiece to enter the throat of the rolls, the component of the friction force must be equal to or greater than component of the normal force, i.e.,

$F \cos \alpha \geq P_r \sin \alpha$

This implies that $\frac{F}{P_r} \geq \frac{\sin \alpha}{\cos \alpha} \geq \tan \alpha$ (2.5)

Since $F = \mu P_r$

Therefore $\mu = \tan \alpha$ (2.6)

If $\tan \alpha > \mu$, the workpiece cannot be drawn.

If $\mu = 0$, rolling cannot occur.

Therefore, free engagement will occur when $\mu > \tan \alpha$ (Dieter, 1988).

2.3 Problems and Defects in Rolled Products

A variety of problems in rolling which lead to specific defects may be on the surfaces of the rolled material and these may arise as a result of interaction of plastically deforming metal with the elastically deforming rolls or may be structural defects within the material. Surface defects may result from inclusions and impurities in the material. Examples include scale, rust, dirt, roll marks and other causes related to the prior treatment and working of the material (Naser and Tom, 2008). Structural defects are wavy edge, zipper cracks in center of the sheet, edge cracks and alligatoring (Naser and Tom, 2008). The problems with shape and flatness are brought about by inhomogeneities in deformation in the rolling direction of the sheet (Naser and Tom, 2008).

Wavy edges are caused by bending of the rolls; the edges of the sheet are thinner than the center which tends to elongate more. Since the edges are restricted by the material at the center, they tend to wrinkle and form wavy edges. Center and edge cracks are caused by low material ductility and barreling of the edges. Alligatoring is a complex phenomenon resulting from inhomogeneous deformation of the material in the rolling direction, and

from any metallurgical weakness along the center line of the original cast ingot, such as piping. Residual stresses are also considered as a major defect in rolling. Schematic illustrations of typical defects in rolling are shown in Figure 2.6.

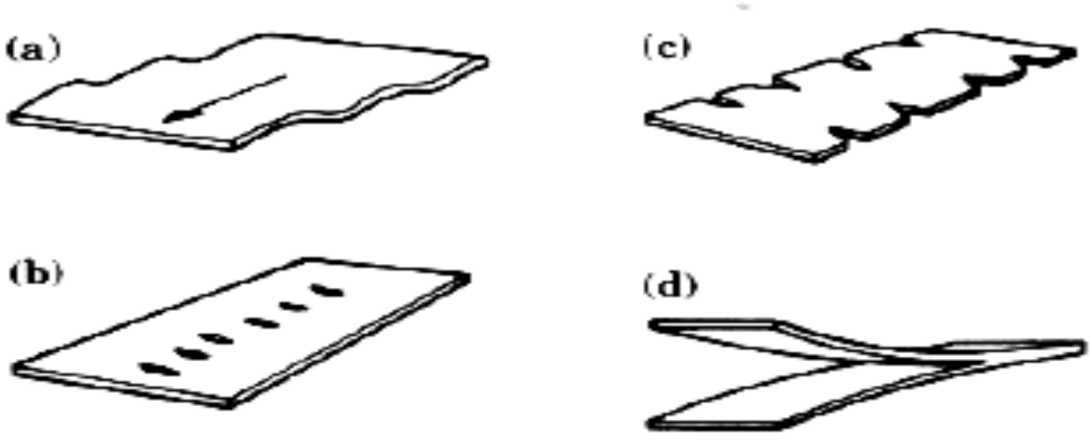


Figure 2.6: Schematic illustration of typical defects in flat rolling (Naser and Tom, 2008).

(a) Wavy edges (b) Zipper cracks in center of strip (c) Edge cracks (d) Alligatoring

2.3.1 Edge Cracking

In rolling process, as the workpiece passes through the rolls, all elements across the width experience some tendency to expand laterally (in the transverse direction of the sheet). The tendency for lateral spread is opposed by transverse friction forces. Due to the friction hill, these are higher toward the center of the sheet so that the elements in the central region spread much less than the outer elements near the edge. The thickness decrease in the center of the sheet goes into a length increase, while part of the thickness decrease at the edges goes into lateral spread; the sheet may develop a slight rounding at its ends. Since there is continuity between the edges and center, the edges of the sheet are strained

in tension, a condition which leads to edge cracking (Dieter, 1988). Figure 2.6c shows a schematic illustration of edge cracking defect.

2.3.2 Causes of Edge Cracking

Edge cracking- a major industrial problem in rolling process- has been attributed to the limited ductility of the rolled material, uneven deformation at the edges (bulging and concave edge) and variations in stress along the width of the rolled material, particularly near the edges (Schey, 1966).

i. **Limited Ductility**: Edge cracking is normally associated with limited ductility which may be due to a number of causes, such as lattice structure with insufficient number of slip planes, or the presence of segregations or constituents of limited ductility or low melting point (Schey, 1966).

   It has been observed by Sansome (1975) that for the rigid rectangular roll gap, strain at edge must have a smaller numerical value than strain at the centre i.e. the material is extended more at the centre than it is at the edge. Should the material be brittle, edge cracking will occur with partial relief of the residual internal stress. However, if the material is ductile the strip will not edge crack, and on emerging from the deformation zone, it will be subjected to the idealized residual stress distribution (Sansome, 1975).

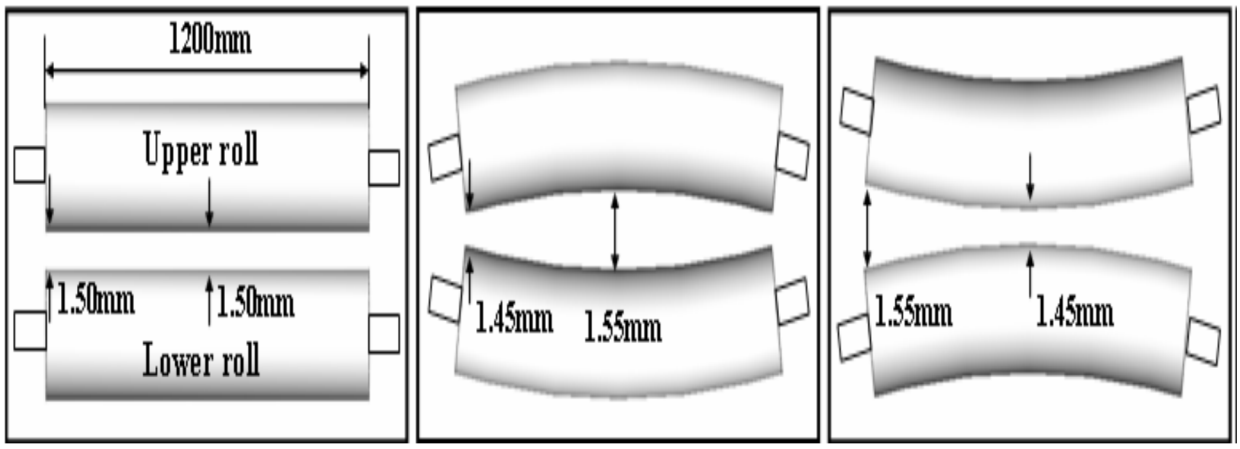
ii. **Uneven Deformation Caused by Roll Bending**: When rolling a relatively thick slab with light reductions i.e. when the rolling condition is such that only the surface of the workpiece is deformed, the deformed zone penetrates to a fraction of the total thickness only (Dieter, 1988). The surface of the slab deforms in all directions and laterally, while the centre remains at unchanged width. In further passes, the ‘over

hanging' material is not directly compressed but is forced to elongate by the bulk deformation of neighbouring material closer to the center. Thus it is subjected to high tensile stresses which lead to cracking in a material of limited ductility (Schey, 1966). When the slab is relatively thin and the pass reduction is heavy so that the deformation extends through the thickness of the sheet, the edges barrel and are forced to elongate by the dragging effect of the bulk material; again, resulting in edge cracking of material with limited ductility (Schey, 1966).

Na and Lee (2008) reported that flatness of the work roll leads to much less probability of the creation of edge crack. They also suggested that intermediate roll shifting; adjustment of back-up roll crown and intermediate roll bending force might be effective method to draw the work roll flat.

Even a four high rolling mill where small diameter work rolls are backed by larger rolls to prevent the deformation of work rolls, bending of work rolls still occurred. Work roll under the action of the rolling force is bent elastically and this roll bending leads to uneven thickness across the width of the strip or to a wavy edge on both sides of the strip. If excessive tension is applied to strip with wavy edge, the crack might propagate sideward of the strip (Na and Lee, 2008).

The research findings of Na and Lee (2008) illustrated three possible deformation modes of work rolls which might occur during cold rolling. These are no bending, negative bending and positive bending as shown in Figure 2.7. In actual rolling process, the state of no bending does not exist. Negative bending and positive bending occur consecutively during rolling.



(a) No bending (b) Negative bending (c) Positive bending

Figure 2.7: Possible elastic deformation mode of work rolls during cold rolling (Na and Lee, 2008).

iii. **Lateral Spread**: It is known from the theory of rolling that in the flat rolling of material, the roll interface pressure changes not only along the arc of contact but also along the width of the sheet (Schey, 1966). While essentially plane-strain condition prevail in the central portions of the rolled slab or sheet, lateral flow (spread) is bound to develop near the edges. This results in a gradual drop of interface pressure toward the edges which lead to the appearance of third component of stress and the plane-strain condition is no longer applied (Schey, 1966).

Employing photoplasticity techniques, Oyinlola (1976) examined the three dimensional strain distributions in rolled billet using a 70:30 Laminac mixtures (flexible and rigid resins). He demonstrated that 70:30 Laminac mixtures when deformed at 51^{o}C simulates the characteristics of aluminium when deformed at 425^{o}C. The distribution of principal shear strains determined from the fringe pattern of rolled blocks of photoplastic material exhibited features which could be related to edge contours known to form during hot-rolling of aluminium (Oyinlola, 1976). According

to his research finding, at 20% deformation, the plane strain assumption no longer held for the particular size of block considered and he concluded that, edge cracking is due to the appearance of third component of strain at higher deformation.

Ghosh *et al.* (2004) concluded that the inception of damage (edge cracking) in the cold rolling process is a three dimensional phenomenon that requires a 3D analytical model for accurate predictions. Therefore the edges of the strip deform longitudinally only because they are bodily attached to the bulk of the strip and yielding is initiated by the combination of compressive and secondary tensile stresses. Therefore tensile stresses are again responsible for edge cracking, even if the edge does not show any concavity or barreling (Schey, 1966).

2.4 Friction and Lubrication in Metal Working Processes

The most obvious effect of friction in general is that work has to be expended which would not otherwise be necessary. This is true in metalworking processes. The higher the friction, the greater the load required to produce a particular deformation. Friction is however advantageous in some aspects. In rolling of a flat strip, the rolls will skid if the friction is too low, and it is necessary to use a relatively poor lubricant to obtain the greatest possible reduction per pass. Apart from increasing external forces, frictional stress has an important influence on metal flow, and may cause serious inhomogeneity in the worked product, as well as surface cracks and other defects (Atkins, 1974).

Friction and lubrication are of vital importance in most metal forming operations. Effective lubrication systems result in low friction levels which reduce the loads imposed on tooling and workpiece as well as edge cracking defect. This can eliminate the problem

of tooling or workpiece failures or permit a reduction in the number of steps required to form a part.

2.4.1 Mode of Lubrication in Cold Rolling

In industrial metalworking, there are two basic modes by which lubricants decrease friction (Atkins, 1974). These are hydrodynamic and boundary lubrications

i. Hydrodynamic Lubrication

The first is by hydrodynamic lubrication which means that a reduction in friction is achieved by maintaining a constant fluid film between solid surfaces. When fully separated, the resistance to motion is only due to the interposed fluid layer. The lubricity of this fluid depends on the area of the film, the rate of shear and the viscosity of the lubricant.

ii. Boundary Lubrication

The second mode is by boundary lubrication. This is when metal to metal contact inevitably occurs. Boundary lubrication typically has a higher coefficient of friction and does allow wear to occur, although it is greatly reduced.

As in most metalworking processes, the main reason for the use of lubricant in the cold rolling process is to control friction and surface quality. Under most circumstances, steel and aluminium are lubricated in such a way that asperities will touch and carry part of the load, causing additional friction (Lugt *et al.,* 1993). If the running surfaces are completely separated by a lubricating film, “hydrodynamic pits” may be formed, resulting in a dull surface, whereas if the lubrication mechanism is of mixed type, the bright surface of the rolls is printed on the strip (Lugt *et al.,* 1993).

In the mixed lubrication situation, friction is caused by both viscous shear in the lubricating film and shear between the touching asperities (Lugt *et al.,* 1993). Low friction reduces the rolling force, which again reduces the elastic flattening of the work rolls and enables a larger reduction with reduce edge cracking defect. However, if the friction is too low the rolls will skid and strip will no longer be drawn through the rolls bite (Atkins, 1974).

2.4.2 Evaluation of Lubricants in Cold Rolling by Plane Strain Compression Test

Before oil can be used as a lubricant in metal working operation, a thorough evaluation of its performance characteristics is necessary. Without a good knowledge on the effective performance of lubricants used, it is often impossible to assess the efficiency of the metal working processes. John (1970) enumerated a number of attributes of metal working lubricants some of which are controlled friction, reduced wear, avoidance of metal pickup on the surface, cooling, protection of old and new surfaces, compatibility with die and workpiece, durability of lubricant film, rapid response, controlled stability and harmless residues. In the assessment of any lubricant, it is therefore necessary to perform laboratory tests which duplicate as closely as possible the conditions found in commercial metal working operations. For this reason, plane strain compression test also known as Watts-Ford Test, is usually used to simulate material behaviour in thermomechanical processes such as rolling (Sutchiffe *et al.,* 2002).

Gaminana (2011) assessed the evaluation of Neem seed, Tiger nut and False Walnut oils as metal working lubricants on the basis of plane strain compression test. An experimental investigation of the tribology during plane strain compression of aluminium strip using

steel tools under formulated lubricant containing ester, hexadane and stearic acids was performed by Sutchiffe *et al.* (2002). Agwandas (1988) work on the evaluation of local oils for cold rolling operation of aluminium sheets using plane strain compression test. Stress strain behaviour of magnesium alloy A231 in plane strain compression test was studied by Ikuo *et al.* (2005) under two lubrication conditions. Hosford (1966) adopted a plane strain compression test to investigate the work hardening of aluminium crystals being deformed by multiple slip. The numerical prediction and experimental measurement of the distribution of strain in plane strain compression tests of AA 5182 by means of grid insert was investigated by Boldetti *et al.* (2006).

In plane strain compression test, a flat strip is compressed between flat parallel platens where the strip is thin compared with the width of the tool; deformation is approximately homogenous in the bite. As long as the width of the strip is large compared with the thickness of the tool, spread is small and plane strain condition apply (Sutchiffe *et al.,* 2002). These conditions are similar to those pertaining in cold metal rolling justifying the use of such test to model rolling process. The dimension of the specimen and the tool must satisfy the following conditions.

$w > 5h$ and $b > 2h$ to $4h$

where w = width of the strip, h = thickness of the strip and b = thickness of the tool (Rowe, 1968).

The reduction capacities of the oils are being investigated base on the reduction in thickness of the material obtained after the test using the formula given below. A schematic diagram of the plane strain compression test is shown in Figure 2.8.

Percentage thickness reduction = ——————————— X100% 2.7

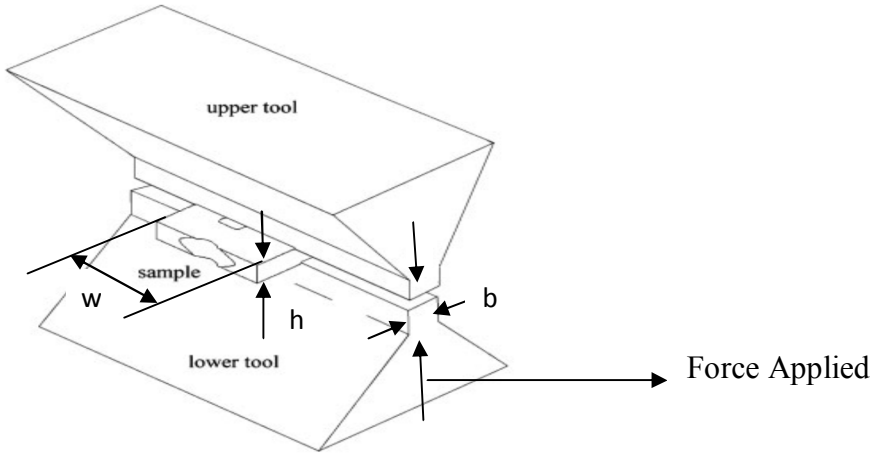


Figure 2.8: A schematic diagram of the plane strain compression test (Boldetti *et al.* 2006).

2.4.3 Chemical Analysis of Lubricating Oils

Fatty oils are polar substances having very long carbon chains with one or more chemically active or polar groups at one end. Both the chemical and physical properties of the oil are determined by their fatty acid radicals which may contain some saturated (unreactive) and unsaturated (reactive) acids. The unsaturated fatty acids are the polar groups that adhere strongly to the workpiece and tool surfaces, causing long chain to be oriented at approximately right angles to the metal surfaces (Babaagba, 1986). These oriented films of polar substances, which are several molecules thick, minimize metal-to-metal contact and friction there by reducing wear. The relative amount of the polar substances in fatty oils has been found to be a measure of degree of unsaturated fatty acids in the oil (Babaagba, 1986).

The saturated fatty acids contents of the local oils are caproic, caprylic, capric, lauric, myristic, palmitic, stearic, arachidic, behenic and linoceric acids (Lugt *et al.,*1993). However, with the presence of carboxylic groups, these acids help in maintaining a strong molecular adherence of the fatty oils to metal surface thereby minimizing friction. The unsaturated fatty acid contents are the oleic and linoleic acids. These acids by themselves are reactive in addition to the presence of carboxylic groups. They therefore contribute more to the molecular adherence of the oils onto the metal surfaces. Ordinary mineral oils likes paraffin does not have this polar (reactive) group because they are chain structure that is in equilibrium which is usually described as saturated molecules.

Dave (1995) stated that polar group such as C_{12}-C_{18} saturated fatty acids or alcohol provide a better boundary lubrication when the fluid film were too thin to provide hydrodynamic lubrication. He also affirmed that the fatty acids tend to be more effective since they can react with oxides surfaces on the metal to form soap. Saponification value of rolling oil directly affects its lubricating property. The higher the saponification value the better the lubrication property of the oils (Dave, 1995). The formation of soap on the metal surfaces during rolling also helps in minimizing friction by the formation of adherence layer which separate the workpiece from the rolls.

2.5 Effect of Iron on Aluminium Alloys

Based on previous research works highlighted as follow, the difficulty of controlling the edge cracking was traced to detrimental effect of the alloying elements in the commercial aluminium alloy under investigation. Specifically, the detrimental effect of iron in aluminium alloys has been traced to the formation of intermetallic phase particles of

various types (Zhang, 2007). Ductility is seriously affected negatively by the presence of the intermetallic phase particles.

Fang *et al.* (2011) investigated the effect of intensive forced melt convection on the mechanical properties of Fe-containing Al-Si based alloys. They observed that as the equilibrium solid solubility of Fe in the Al solid solution (α-Al) is low, Fe exists in Al-alloys in the form of Fe-bearing intermetallic compounds. In commercial Al-Si based cast alloys, these compounds are often of the morphologies, either as long needles or large plates, which drastically reduce the ductility of the alloys.

John (2009) worked on the effect of iron in Al-Si casting alloys and concluded that wherever possible, iron level in Al-Si alloys should be kept at the bearable minimum level in order to avoid the detrimental effect on mechanical properties, particularly ductility and fracture toughness.

Based on the investigation of Caceres *et al.* (2003) on Al-SiCuMg alloy, an increase in iron content between 0.2% and 0.8% led to the reduction in ultimate tensile strength by 15% and ductility by 50% while the hardness increased by 12%. These variations are due to the presence of the needle-like structures that provide a brittle behaviour of the alloy.

Investigation on higher level content of iron in Al-SiCu alloy by Tang and Sritharan (1998) revealed that, by changing the iron content from 1 up to 1.8% successively resulted in a serious reduction in tensile strength as well as the ductility. However, the hardness and yield strength increase slightly.

Lu and Dahel (2005) observed that at low iron level contents (Fe<0.3%), sponge-like pores have been detected in the center of casting. This has been suggested to be formed by

the presence of ternary β-platelets. Between the range content of 0.3% and 0.7%, the levels of porosities in the alloy would have been distributed across a wider area. The precipitation of binary β-phases is proposed to block the feeding channels of the interdendrites network. Chemically, this detrimental effect can be minimized by limiting the maximum content of the Fe impurity, or by alloying with other element such as manganese (Lu and Dahel, 2005).

In order to enhance the overall properties such as tensile strength, fatigue and corrosion, it is required that the morphology of the iron-rich β-Al_5FeSi-needles be altered to be more compact, less harmful intermetallic compounds such as α-$Al_{15}(Fe,Mn)_3Si_2$ having a Chinese script morphology (Seifeddine and Svensson, 2009).

Shabestari *et al.* (2002) reported that alloying with 0.9%Mn, resulted in apparent fragmentation of the β-Al_5FeSi-needles. At higher Mn levels, the plate-like morphology of the β-Al_5FeSi-needles was replaced by α-$Al_{15}(Fe,Mn)_3Si_2$-dendrites in the form of plate, polyhedral or star-like shape.

2.5.1 Effect of Iron on the Mechanical and Structural Properties of Aluminium Alloys

Commercial aluminium alloys always contain iron, often as undesirable impurity and occasionally as a useful main alloying element. As a minor alloying element, iron has been used occasionally in; Al-Cu-Ni alloys to enhance high temperature mechanical properties, Al-Mg alloys to reduce coarsening, Al-Fe-Ni alloys to enhance corrosion resistance in steam environment, and in high pressure die-cast Al-alloys to facilitate ejection and to help in die-release (Fang *et al.,* 2011). It should be noted that iron does not always exert a negative influence; in certain wrought aluminium alloys (i.e. alloys used in forged,

extruded or rolled forms), iron can be a deliberate alloying addition to improve the processing capabilities of the alloy and/or the strength of the final wrought product (John, 2009).

In industrial practice, the iron pickup results mainly from the use of steel tools as stirrer during melting and casting, and the use of scrap materials. For the vast majority of Al-alloys, the presence of iron is detrimental to the mechanical properties (Taylor *et al.*, 1999). Iron pickup is thus a major problem for industrial use and recycling of Al-alloys.

Although iron is highly soluble in liquid aluminium and its alloys, it has very little solubility in the α-Al solid (0.05wt %), and so it tends to combine with other elements to form intermetallic phase particles of various types (John, 2009). In the absence of silicon, the dominant phases that form are Al_3Fe and Al_6Fe, but when Si is present, the dominant phases are Al_8Fe_2Si (known as alpha- or α-phase) and Al_5FeSi (known as beta- or β-phase). If Mg is also present with Si alternative phase called pi- or π-phase can form $Al_8FeMg_3Si_6$ (John, 2009). Another common phase that forms when Mn is present with Si is $Al_{15}(Fe,Mn)_3Si_2$, also confusingly known as α-phase (John, 2009). This phase tends to form in preference to other α-phases whenever Mn is present. There are also other rarer phases which form when other elements are present, e.g. Ni, Co, Cr, Be. When these low symmetry compounds crystallize, (in particular as primary phase during solidification) they are prone to grow into long needles/plates that are extremely detrimental to both strength and ductility (Zhang, 2007).

Mbuya *et al.* (2003) have extensively reviewed the effect of iron on the mechanical properties of Al-alloys and they consistently reported that as iron level increases, the

ductility of Al-Si based alloys decreases. This is usually accompanied by an increase in tensile strength, however, the yield stress become unaffected by iron, unless the ductility is affected so much that the alloy cannot even reach yield before brittle fracture occurs. The detrimental effect of iron begins at quite low primary Fe levels (0.052 wt %) but becomes far more serious once a critical Fe level (dependent on composition) is exceeded (John, 2009). The detrimental effect of iron is due to two main reasons (Siddiqui *et al.,* 2000).

i. The size and density of iron-containing intermetallic phase particles increases with iron content, and since this participates directly in the fracture mechanism, the more intermetallic there are, the lower the ductility.
ii. As iron level increases, porosity increases, and this defect also has an impact on ductility.

The critical iron level is directly related to the silicon concentration of the alloy as shown in Figure 2.9. The point of intersection with line AB is where the formation of β-phase platelets started to occur before the formation of eutectic at B (John, 2009).

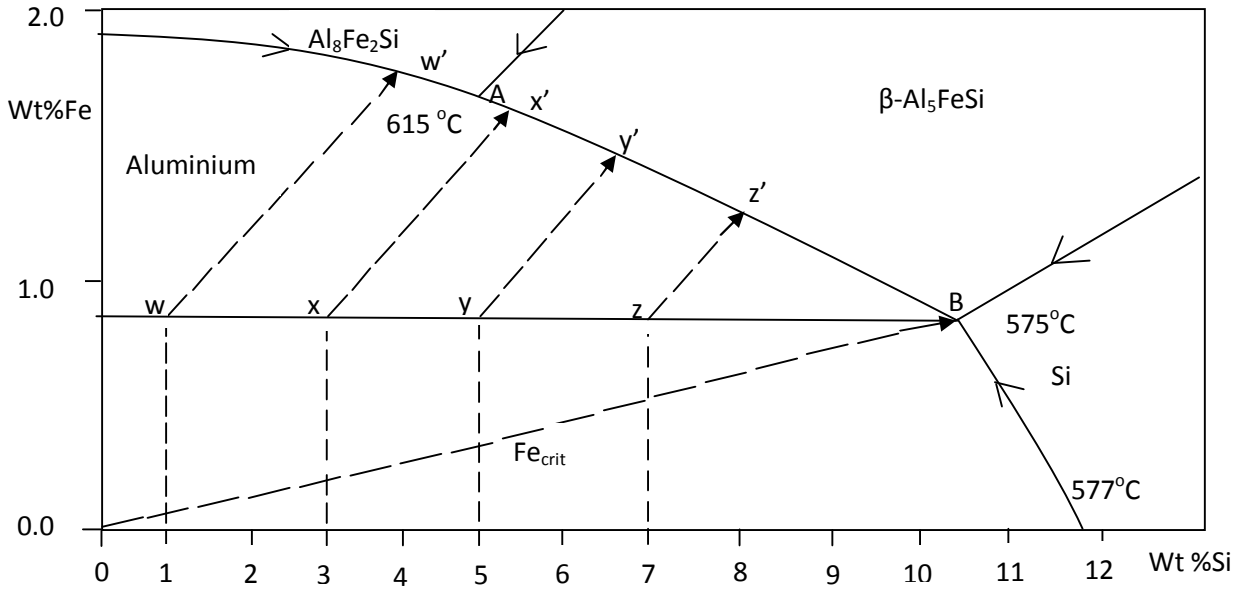


Figure 2.9: Ternary Al-Si-Fe phase diagram of primary Al solidification paths for all alloys with Fe_{crit} iron levels, and 1%Si (w-w'), 3%Si (x-x'), 5%Si (y-y') and 7%Si (z-z') alloys with 0.8%Fe.

As the silicon content increases, the amount of iron that can be tolerated before the intermetallic phases start forming increases. At 1%Si, the critical iron content is ~0.1%, at 3%Si, it rises to ~0.2%, at 5%Si, it is ~0.35%, and at 7%Si, it reaches ~0.5% (John, 2009).

In many instances, however, the effect of iron on the ductility of an alloy is not so clearly demarcated because as the Fe level increases above Fe_{crit}, the cooling becomes slower and/or there are lots of casting defects present, the ductility tends to drop to extremely low levels, <1%, and sometimes tensile specimens break even before yielding i.e. <2% (John, 2009).

The reason why the Fe-containing intermetallic particles are detrimental to an alloy's mechanical properties is that they are much more easily fractured under tensile load than the aluminium matrix or the smaller silicon particles (if modified); micro-cracks tend to initiate at these particles and they provide easy pathways for micro-crack to propagate (Kuijpers *et al.,* 2003).

Tajally *et al.* (2009) investigated the effect of cold rolling on bending and tensile behaviour of 7075 aluminium alloy and observed that after 58% cold working, there was a rapid increase in yield strength of 119.25% due to high density of dislocations. In addition, increases in the tensile strength and hardness value with decrease in percentage elongation of the rolled material were observed.

Schey (1966) performed experiment aimed at preventing edge cracking on aluminium-8% magnesium alloy and on iron powder bodies. It was revealed that restraining bars guided in and supported by grooves machined in to the rolls, moved together with the slab thereby preventing its spreading. While the concept has proved a feasible means of eliminating edge cracking in cold rolling of aluminium alloys, the restraining technique is cumbersome.

In view of the detrimental effect of iron to the ductility of the aluminium alloys, an optimum value of iron which will improve the processing capabilities and strength without any negative effect to the ductility of the alloy and the most effective lubricant that will reduce the frictional effect in cold rolling of the alloy will help in minimizing edge cracking defect in cold rolling operation. These two factors have been quantitatively determined in this research work as a means of edge cracking reduction in cold rolling operation of aluminium alloy 8011.

CHAPTER THREE

3.0 MATERIALS, EQUIPMENT AND GENERAL EXPERIMENTAL PROCEDURES

3.1 Introduction

In this chapter the materials used in this study are listed and the equipments used are described. The methodology of the study are explained in detail ranging from casting of the alloy and cold rolling operation followed by testing of mechanical properties. The procedure for the metallographic examination, chemical analysis of the investigated oil and plain strain compression test were also described.

3.2 Materials

The materials used in this research work include;

3.2.1 Commercial Aluminium Alloy 8011

The commercial aluminium alloy 8011 has the following ranges of chemical composition as shown in Table 3.1.

Table 3.1: Chemical composition of commercial aluminium alloy 8011.

Elements	Al	Fe	Si	Mn	Cu	Mg	Ti	Zn	Cr	Pb
Composition (%)	97.3-98.9	0.6-1.0	0.5-0.90	≤ 0.20	≤ 0.10	≤ 0.05	≤ 0.08	≤ 0.10	≤ 0.05	≤ 0.05

(Ullrich Aluminium Company Technical Report on Chemical Composition of Aluminium Alloys, 2008).

The chemical composition of as-received (1300mm x 240mm x 7mm) commercial aluminium alloy 8011 from Tower Aluminium Rolling Mills is shown in Table 3.2.

Table 3.2: Chemical composition of as-received commercial aluminium alloy 8011.

Elements	Al	Fe	Si	Mn	Cu	Mg	Ti	Zn	Cr	Pb
Composition (%)	98.183	0.857	0.551	0.117	0.072	0.020	0.015	0.120	0.050	0.015

3.2.2 Mixed Coconut/diesel and Neem Seed Oil

The mixed coconut/diesel oil being used as a commercial lubricant in the cold rolling of AA 8011 was obtained from Tower Aluminium Rolling Mills. The neem seed oil being investigated as an alternative lubricant in cold rolling of AA 8011 was obtained from National Research Institute for Chemical Technology (NARICT), Zaria. Coconut and diesel oils used as laboratory formulated oil were sourced locally.

3.3 Equipment

The rolling mill used in this research work was four-high commercial flat rolling mill located at Tower Aluminium Rolling Mills. The chemical analysis of the alloys was conducted in the same company using Optical Emission Spectrometer. Gas Chromatography Mass Spectroscopy (GCMS) that was made available at National Research Institute for Chemical Technology, Zaria was used to analyze the composition of the oils used in this research work. Compression test was conducted on 500KN Universal Compression Testing Machine while tensile and hardness tests were carried out respectively on a Hounsfield Tensometer and Microvicker Hardness Testing Machine of capacity 5Kgf available at Mechanical Engineering Department, Ahmadu Bello University, Zaria. Impact test and microstructural examination were conducted respectively on a Charpy Impact Testing Machine of capacity 25J and Optical

Metallurgical Microscope available at Metallurgical and Materials Engineering Department, Ahmadu Bello University, Zaria.

3.4 Experimental Procedures

The experimental procedures of this study consist:

3.4.1 Casting of Alloys

The casting was done in the workshop of Metallurgical and Materials Engineering Department, Ahmadu Bello University, Zaria. Three different aluminium alloys of varying iron contents within the range of AA 8011 were produced by melting appropriate quantities of commercial aluminium wires obtained from Northern Cable Company of Nigeria (NOCACO) with other alloying elements appropriately added. These alloys were labeled as alloy A, B and C. Seven samples each of dimension 240mm x 140mm x 7mm were cast per alloy using metal mould. The as-received commercial aluminium alloy 8011 was cut into seven pieces of the same dimension as previously highlighted. This alloy was labeled as alloy AR. The chemical compositions of the alloys are shown in Table 3.3.

Table 3.3: Chemical compositions of as-cast and as-received aluminum alloys 8011

Alloy	Al	Fe	Si	Mn	Cu	Mg	Ti	Zn	Pb	Cr
A	98.332	0.708	0.551	0.117	0.072	0.020	0.015	0.120	0.015	0.050
AR	98.183	0.857	0.551	0.117	0.072	0.020	0.015	0.120	0.015	0.050
B	98.131	0.909	0.551	0.117	0.072	0.020	0.015	0.120	0.015	0.050
C	98.109	0.931	0.551	0.117	0.072	0.020	0.015	0.120	0.015	0.050

3.4.2 Cold Rolling Experiment

A four-high commercial rolling mill consisting of a pair of work rolls and backup rolls was used to carry out cold rolling experiment. The work roll and backup roll were 240mm and 520mm in diameters respectively. The upper rolls were vertically adjustable; such that the roll gap could be set to any desired gap. The two sides of the mill were designated; drive side (DS) and operator side (OP). Two motors on the drive side powered the rolls, which ran at a constant speed of 43rpm.

A total of 24 samples were annealed at 450^{o}C for one hour. Each plate was fed directly between the work rolls, which imposed no forward or back tension loads on the plate. The experiment was performed under mixed coconut/diesel oil used by the rolling mill as lubricant. The investigated rolling schedule is presented in Table 3.4 while the photograph of the flat rolling mill used for the cold rolling experiment is shown in Figure 3.1.

Table 3.4: Investigated rolling schedule

Initial thickness (mm)	Final thickness (mm)	Percent reduction in thickness (%)
7	4.9	30
7	4.2	40
7	3.5	50
7	2.8	60
7	2.1	70
7	1.4	80

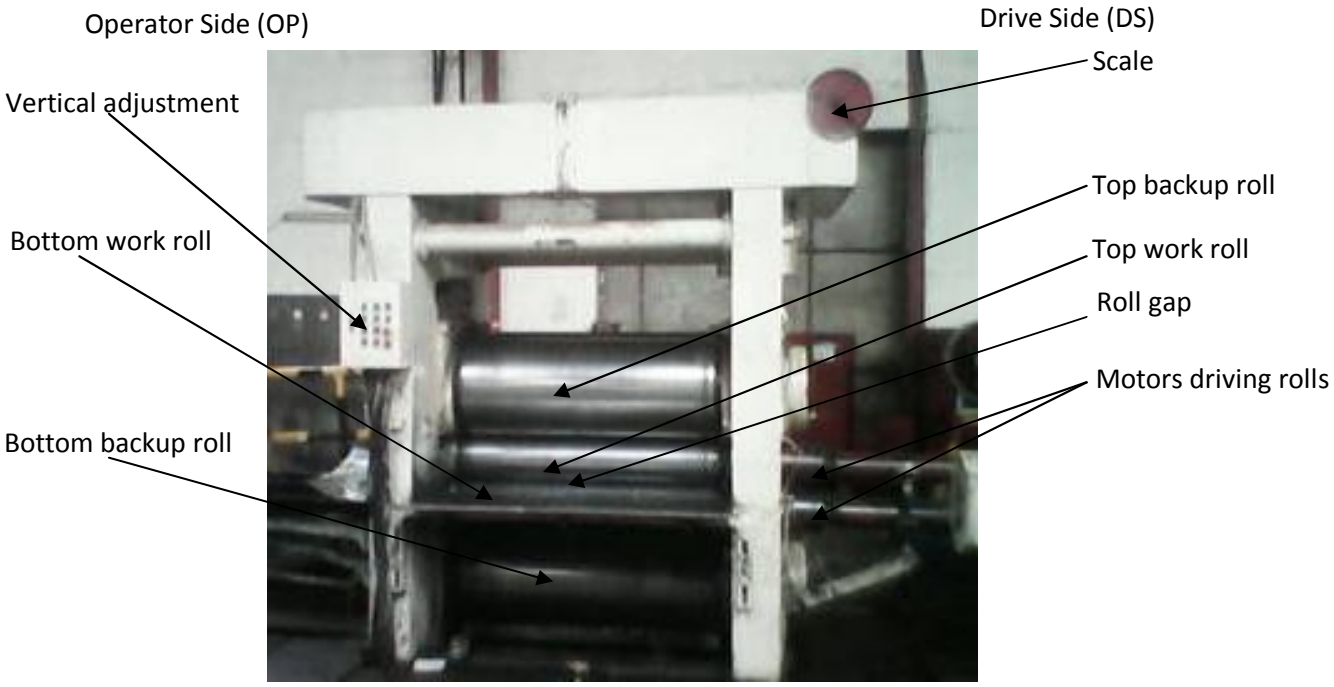


Figure 3.1: Photograph of the flat mill showing various mechanisms

3.4.3 Tensile Strength Test

Tensile strength measurement was conducted on a Hounsfield Tensometer Machine. The tensile specimens were machined from the as-received, as-cast (of varying iron content) and cold-rolled samples oriented along the rolling direction according to ASTM E8M standard. The test piece was locked securely within the grips of the tensometer machine. The tensile force required to stretch the sample was supplied by manually operated screw attached to the machine at constant strain rate until the test piece broke. Extension of the sample was monitored in terms of the relative displacement using the attached pin at the cross-head to punch the graph sheet attached to the tensometer. Consequently, load and extension data available from the graph sheet were converted to specific values of stress and strain. The percentage elongation of the test piece after breaking was determined from

the specimens with the aid of vernier caliper and the results were used to calculate the ductility of the specimens.

3.4.4 Hardness Test

The hardness values of as-received, as-cast (of varying iron content) and cold-rolled samples were determined using Microvicker Hardness Testing Machine according to ASTM E384 standard. An indentor was placed above the sample flat surface. A load of 0.3Kgf was applied on the indentor for about 15-seconds which then penetrates the surface of the specimen. The modern micro indentation hardness testing equipment has been automated by coupling the indentor apparatus to an image analyzer that incorporates a computer and software package. The software controls important system functions including indenting, location of indent spacing, computation of hardness values and plotting of data. The hardness value was red directly from the computer. This procedure was repeated three times for each specimen and the average was taken as the hardness value for the specimen.

3.4.5 Impact Strength Test

The impact strength values of as-received, as-cast (of varying iron content) and cold-rolled samples were determined using Charpy Impact Testing Machine according to ASTM E23 standard. A V-notch was machined into a 10mm wide and 100mm long test specimen. The depth of the notch was 4mm. The specimen was placed across parallel jaw of the testing machine. A heavy pendulum, released from a known height, struck and broke the specimen before it continues its upward swing. This measured the energy necessary to fracture the standard notch specimen by an impact load and the dial pointer of the scale on

the machine indicates the energy absorbed, in Joules, by the specimen from the impact. The values of the energy absorbed in breaking the specimens were recorded.

3.4.6 Metallographic Examination

A total of eight specimens were prepared from the batches of samples (as-cast, as-received and 80% cold-rolled reduction in thickness) for microstructural examination. The specimens were prepared for optical examination by cutting, successive grinding using silicon carbide grit paper of 240, 320, 400 and 600 microns following a standard guide for preparation of metallographic specimens (ASTM E3).

Polishing was carried out on a rotating cloth to ensure mirror-like surface. A solution containing 5ml nitric acid, 2ml hydrofluoric acid and 100ml of distilled water was used to etch the specimens for about 10 seconds according to ASTM E340 standard. The specimens were observed under Digital Metallurgical Microscope with an in-built camera; micrograph of each specimen was recorded at a magnification of 100X.

3.4.7 Chemical Analysis of the Investigated Oils

The fatty acids compositions of mixed coconut/diesel and neem seed oil analyzed using GCMS are shown in Table 4.8. The free fatty acids and the saponification values of the two oils were determined using equipment available in Chemical Engineering Department, Ahmadu Bello University, Zaria. Formulation of an alternative cold rolling lubricant (mixing of the locally sourced coconut and diesel oils in various proportions) was achieved by using facilities provided in Biochemistry Department, Ahmadu Bello University, Zaria. Five different proportions of the mixtures were prepared.

3.4.8 Plane Strain Compression Test

In this work, a plane strain compression test was employed in comparing the performance of mixed coconut/diesel oil (factory rolling oil) with neem seed oil as cold rolling lubricants for AA 8011. The test was conducted on Universal Compression Testing Machine according to ASTM E9 standard. A total of ten plates (five plates for each oil) of dimension 240mm x 40mm x 7mm each were used for the experiment. The platen used is 18mm in thickness. The plates and surface of the platens of compressive testing machine were cleaned with a mixture of methanol and ethanol using cutting wool. Each of the oil under investigation was applied to the surface of both the plates and the platens.

The test on individual oil consists of compressing the plates between the platens with a load of 80kN, 90kN, 100kN, 110kN and 120kN, accordingly, and taking five impressions on each plate, after which the resultant reductions in thickness were measured using a vernier caliper. The variation in thickness is assumed to be related to frictional condition produced by the lubricants (Watts and Ford, 1952). The percentage reductions in thickness were determined.

Performance evaluation of each percentage mixed of locally sourced coconut and diesel oils as lubricant in cold rolling of samples of the aluminium alloy 8011 was quantitatively determined from the plane strain compression test by the percentage reduction in thickness under various oil mixed lubrication conditions. Five samples of the alloy each of dimension 140mm x 40mm x 4.9mm were compressed on a universal compression testing machine with a load of 100kN by taking five impressions for each sample using five

different proportions of oil mixture as lubricant. The dimensions of the samples and the tool satisfied conditions stated in Rowe (1968).

CHAPTER FOUR

4.0 EXPERIMENTAL RESULTS

4.1 Introduction

This chapter shows the results of the mechanical properties of as-received, as-cast and cold-rolled samples at various percent reductions in thickness, microstructural examination of the alloys and chemical analysis of the oils used as lubricant. The result of the lubrication potential of the investigated oil in cold rolling of the alloys by plain strain compression test was also highlighted.

4.2 Evaluated Mechanical Properties

The ultimate tensile strength, percentage elongation, hardness value and impact strength of as-received and as-cast samples of varying iron contents and samples cold-rolled to various reductions in thickness are presented in Tables 4.1.

Table 4.1: Mechanical properties of aluminium alloy 8011

Samples	Reduction in thickness (%)	Ultimate tensile strength (MPa)	Elongation (%)	Microvicker hardness (HV)	Impact Strength (J)
As-cast 0.708%Fe	30	130.31	8.00	8.7	18.00
	40	161.75	13.25	9.9	15.00
	50	169.63	13.00	10.9	8.40
	60	171.45	12.50	11.4	2.80
	70	161.00	11.75	11.8	2.50
	80	115.00	9.50	11.6	1.25
As-received 0.857%Fe	30	138.89	15.50	10.9	19.35
	40	142.53	17.50	11.4	10.70
	50	162.23	13.50	11.8	7.80
	60	176.45	12.25	12.1	4.50
	70	149.48	11.75	11.8	3.90
	80	130.00	10.20	10.7	1.35
As-cast 0.909%Fe	30	130.21	8.25	10.1	10.70
	40	146.84	13.50	11.2	9.60
	50	162.54	12.00	12.6	7.50
	60	161.54	11.75	12.4	3.00
	70	155.00	9.25	12.2	2.70
	80	163.16	7.00	12.0	1.40
As-cast 0.931%Fe	30	135.31	9.75	11.0	9.80
	40	157.36	14.75	12.2	7.40
	50	156.35	9.50	11.5	6.60
	60	167.35	8.50	11.2	3.80
	70	132.65	7.00	11.1	3.75
	80	170.00	8.50	10.9	1.45

The stress-strain curves for the as-received, as-cast and cold-rolled samples at various reductions in thickness are shown in Appendix B, Figures B1 – B7.

4.3 Microstructural Examination of AA 8011

The micrographs of as-received, as-cast (of varying iron contents) and cold-rolled samples under various investigated conditions are presented in Appendix C, Plates C1 and C2.

4.4 Chemical Analysis of the Investigated Oils

The chemical composition of the investigated oils used as lubricants for friction reduction in cold-rolled commercial AA 8011 is appended in Table 4.2 below:

Table 4.2: Fatty acids composition of the investigated oils

Fatty Acids			% composition of Investigated oils	
Type	Chain length	Double bond	Neem seed oil	Mixed coconut/diesel oil
Myristic	14	0	1.33	-
Palmitic	16	0	17.21	-
Stearic	18	0	15.23	-
Oleic	18	1	49.46	1.38
Linoleic	18	2	16.77	-
Percentage un-saturation			66.23	1.38

Table 4.3: Saponification value and free fatty acid of the investigated oils

Lubricating oil	Chemical composition	
	Saponification value ($mgKOHg^{-1}$)	Free fatty acid (%)
Neem seed oil	180.92	23.12
Mixed coconut/diesel oil	25.25	4.23

4.5 Lubrication Potential of the Investigated Oils in Cold Rolling of AA 8011 by Plane Strain Compression Test

The lubrication capacities of mixed coconut/diesel oil and that of neem seed oil in cold rolling operation of commercial aluminium alloy 8011 assessed by plane strain compression test are presented in Table 4.4. The percentage reductions in thickness obtained by mixing coconut oil and diesel in different proportions as lubricant under a compressive load of 100kN are given in Table 4.5.

Table 4.4: Performance evaluation of mixed coconut/diesel and neem seed oils in cold rolling of as-received AA 8011 assessed by plane strain compression.

Applied reduction load (kN)	Initial thickness (mm)	Final thickness (mm)		Percentage reduction in thickness (%)	
		Coconut/diesel oil	Neem seed oil	Coconut/diesel oil	Neem seed oil
80	7	6.71	6.54	4.14	6.57
90	7	6.48	6.40	7.43	8.57
100	7	6.18	5.31	11.71	24.14
110	7	5.26	4.68	24.86	33.14
120	7	4.58	3.60	34.57	48.57

Table 4.5: Performance evaluation of mixed oil lubricant in various proportions (coconut and diesel oils) in cold rolling of as-received AA 8011 assessed by plane strain compression test.

Oil sample	Initial thickness (mm)	Final thickness (mm)	Percentage reduction in thickness (%)
P	4.9	4.03	17.76
Q	4.9	3.85	21.43
R	4.9	3.80	22.45
S	4.9	3.88	20.82
T	4.9	3.98	19.18

Oil samples: P- 80%D:20%C, Q- 75%D:25%C, R- 70%D:30%C, S- 65%D:35%C and T-60%D:40%C, where D represents Diesel oil and C represents Coconut oil

CHAPTER FIVE

5.0 DISCUSSION OF EXPERIMENTAL RESULTS

5.1 Introduction

This chapter discusses extensively the experimental results of this study. It consists of edge cracking characteristics of aluminium alloy 8011 at various cold-rolled reductions in thickness, effect of iron content on the mechanical properties and microstructure of the aluminium alloy 8011. Evaluations of lubricants in cold rolling process and proportions of mixture of coconut and diesel oil in cold rolling process were also discussed.

5.2 Edge Cracking Characteristics of Aluminium Alloy 8011 of Varying Iron Contents Cold-rolled to Various Reductions in Thickness

The visually examined edges of as-cast and as-received samples of alloy containing 0.708%Fe and 0.857%Fe respectively that were cold-rolled to various percent reductions in thickness revealed no edge cracking propensity for all the reductions percentage investigated. The as-cast samples of the alloy containing 0.909%Fe and 0.931%Fe cold-rolled to various percent reductions in thickness revealed no edge cracking tendency up to 60% reduction in thickness. However at 70% and 80%, evidence of edge cracking became very prominent in the rolled samples.

In general, aluminium alloy 8011 containing 0.9%Fe and below can be cold-rolled without any edge cracking defect. Above 0.9%Fe, the alloy could be successfully cold-rolled to 60% reduction in thickness without emergence of edge cracking. However edge cracking defect became inevitable in AA 8011 samples containing more than 0.9%Fe when cold-rolled to 70% and 80% reductions in thickness.

The emergence of edge cracking defect of the cold-rolled samples containing above 0.9%Fe could be attributed to the high level of intermetallic particles which are also being revealed in the micrographs of as-cast samples of AA 8011 of Plate C1 in Appendix C and this is in agreement with the work of Zhang (2007). The combined effect of rolling operation and intermetallic particles could lead to complicated array of different kind of defects such as high dislocation density. It is evident that with increasing density of dislocation, ductility decreases due to lower rate of dislocation movement (Tajally *et al.,* 2009). Furthermore, in rolling operation inclusions and other defects become elongated in the rolling direction; the long grain boundaries in rolled materials can accommodate suitable sites for crack initiation and preferential direction for crack propagation along the long grain boundaries which could lead to edge cracking in the alloys of high iron content at high percentage deformation.

In the present investigation, the visually examined surfaces of the cold-rolled samples containing high level of iron after being cold rolled to 70% and 80% reductions in thickness revealed similar trend of edge cracking propensity as shown in Plates A5 and A6 of Appendix A.

5.3 Effect of Iron Content on Tensile Properties of Cold-rolled Samples of AA 8011

It can be deduced from Figure B1 (Appendix B) that the as-received sample AR has the highest tensile strength. This is closely followed by as-cast samples A, B and C in descending order of magnitude. The precipitated intermetallic phases Al_mFe and $Al_xFe_ySi_y$ accompanied the water-cooled twin-roll casting process (increased speed of crystallization and simultaneous hot rolling in semi-solid state) should have contributed to the high level

of tensile property obtained in as-received sample and this affirmed the research finding of Varuzan *et al.* (2005).

The low tensile properties revealed in sample C could be attributed to the morphology of formation of intermetallic phases of iron-rich β-phase (Al_5FeSi) that promotes the deterioration of strength and ductility, consequently promoting the initiation of cracks under tensile load and this is in agreement with the work of Fabia *et al.,* (2009). The subjection of this alloy with high concentration of intermetallic phases to tensile loading might have resulted in quick nucleation, growth and coalescence of voids yielding a low tensile strength as obtained in the present investigation.

As revealed in Figures B2 – B7, the tensile strength increases with increasing percent reduction in thickness while the strength decreases with increasing iron content. The reason for the observed trend is that iron-containing intermetallic particles are detrimental to an alloy's mechanical properties because they are much more easily fracture under tensile load and this had been previously reported in the research finding of Taylor *et al.* (2000).

Samples B and C show exceptionally high tensile strengths compared to other samples cold-rolled to 70% and 80% reductions in thickness. While the tensile strengths in sample B and C increased with increasing percent reduction in thickness, sample A and AR displayed a decrease in tensile values with increasing percent reduction in thickness. This implies that alloys with higher iron contents posses higher tensile strength at higher deformation than the alloys of lower iron contents. This might be due to high amount of grain refinement of the intermetallic phases to form fine grain structures during plastic

deformation of the alloys. According to Hall Pitch, (William, 2009) a fine-grained material is harder and stronger than one that are of coarse grain structure, since the former has a greater total boundary area to impede dislocation motion.

These high quantities of intermetallic phase particles present in sample B and C which are reformed into fine grain structures by cold rolling operation might likely be the causes of edge cracking defect observed in the samples at 70% and 80% reductions in thickness as shown in Plates A5 and A6.

5.4 Effect of Iron Content on Ultimate Tensile Strength of Cold-rolled Samples of AA 8011

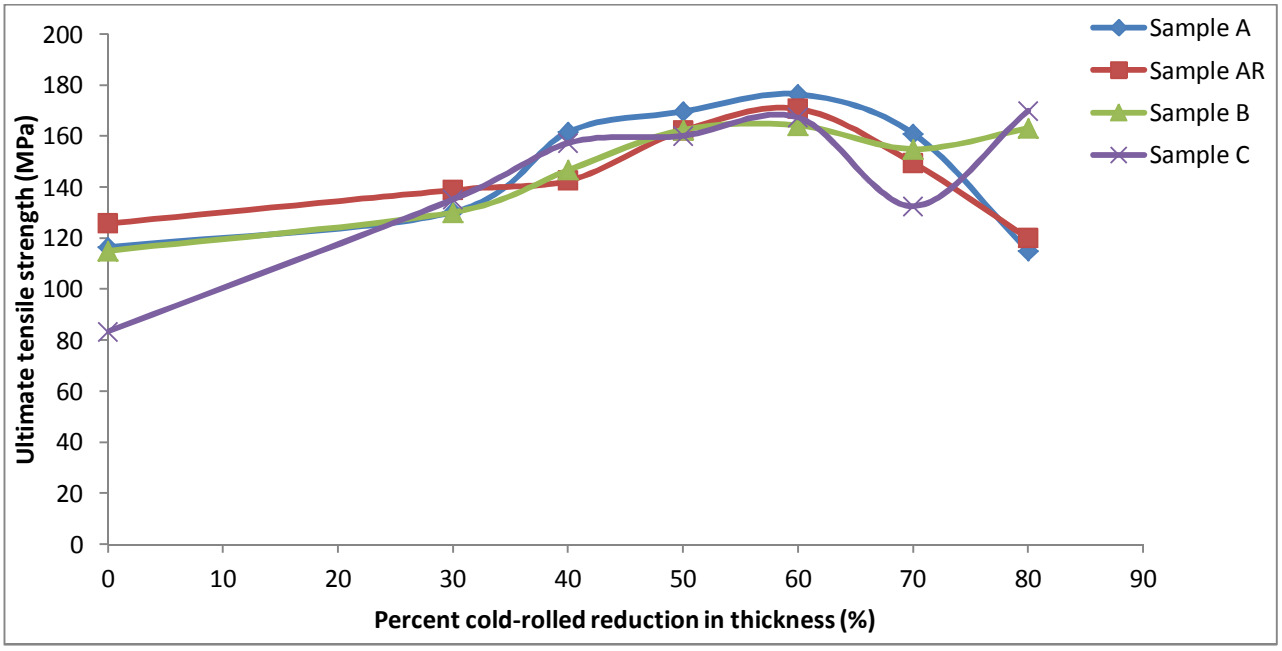


Figure 5.1: Graph of ultimate tensile strength against percent cold-rolled reduction in thickness

Plastic deformation of metals is one of the most important parameters in increasing the mechanical properties of the metals and its alloys. The rapid increase of the values of the ultimate tensile strength of as-received and as-cast samples cold-rolled up to 60%

reduction in thickness could be attributed to the complicated array of defects such as high density of dislocations produced in the alloys during deformation. As previously claimed by Tajally *et al.* (2009), the level of dislocation density is often responsible for variation in mechanical properties such as ultimate tensile strength, ductility and hardness. Dislocations density increases with increasing cold deformation; new dislocations which are created by cold deformation interact with existing one in the material thereby promoting an increase in strength value (Zainul, 2009).

The negative effect of the intermetallic particles becomes less when the size of the intermetallic impurity becomes small (Haga *et al.,* 2008). During cold rolling of the alloys, dislocation density increases as the degree of deformation increases; the fragmentation of interdendritic particles also occur. Due to the interaction of dislocations with each other and with impurities, there is increase in work hardening rate, resulting in an increase in both the strength and hardness values but loss in ductility and this may lead to edge cracking in the alloy of high iron content at higher deformation. It is expected therefore that the ultimate tensile strength will increase with increasing percent reduction in thickness since the intermetallic particles have been broken down by rolling operation.

At 70% reduction in thickness, the ultimate tensile strengths of all the alloys decreased. This might be due to release of stress carried by the second phase particles. When crack occurs in these particles, it affects the overall load bearing capacity of the alloys and hence, it limits its work hardening bebaviour since the flow stress increase in the matrix leads to a higher level of load transfer to the second phase intermetallic particles as have been previously reported by Salem, (2007).

At 80% reduction in thickness, sample B and C show excellent increase in ultimate tensile strength when compared to sample A and AR attributed to high level of grains boundaries in the structure as a result of large quantity of intermetallic particles which fragmented into fine grains by plastic deformation leading to strength increase as explained earlier.

5.5 Effect of Iron Content on Ductility of the Cold-rolled Samples of AA 8011

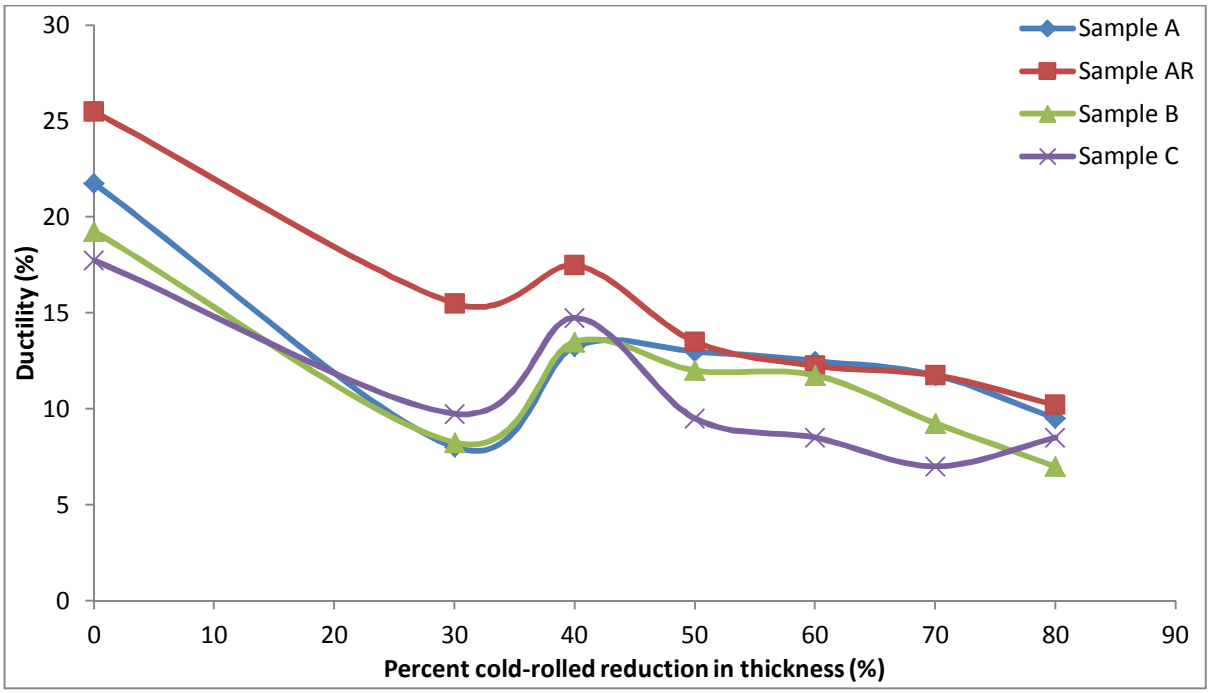


Figure 5.2: Graph of ductility against percent cold-rolled reductions in thickness

The quantitative ductility measure of as-received and as-cast alloy samples subjected to 30% reduction in thickness show rapid decrease in ductility of 63.22%, 39.22%, 57.14% and 45.07% for alloys A, AR, B and C respectively (Figure 5.2). The observed quantitative ductility decreases with increase in iron content. The rapid decrease in ductility is as a result of large immobile dislocation created by the complicated network of interlocking dislocations leading to strength increment and large loss in ductility.

At 40% reduction in sample thickness, rapid increases in ductility for all the alloys were observed. The simultaneous increase in ductility could be attributed to the microstructural changes occurring during deformation process. As reported by Valiev (2003), the main deformation mechanisms were dislocation movements and twining for coarse grains materials. In ultrafine grained materials, the grains with high grain boundaries impeded the motion of dislocations and hence improved the strength of the materials and at the same time, the ultrafine grains formed during deformation might facilitate an increase in grain boundary sliding and hence grain rotation which could improve ductility (Akshay and Ibrahim, 2008). The increase in ductility therefore should have been linked to grain boundaries sliding as observed in the research finding of Akshay and Ibrahim, (2008).

Above 40% reduction in sample thickness, the ductility levels of all the samples decreased drastically both with the increasing percent reduction in thickness and level of iron content. The general decrease in ductility might be due to dislocations generation which interacted and impeded each other and hindering their motion, thereby decreasing the ductility of the alloys. Samples B and C exhibited lower ductility at 70% and 80% reductions in thickness when compared to other samples. This decrement in ductility could contribute to edge cracking observed in the alloys at higher percent reductions in thickness as shown in Plates A5 – A6 of Appendix A.

5.6 Effect of Iron Content on Hardness Properties of Cold-rolled Samples of AA 8011

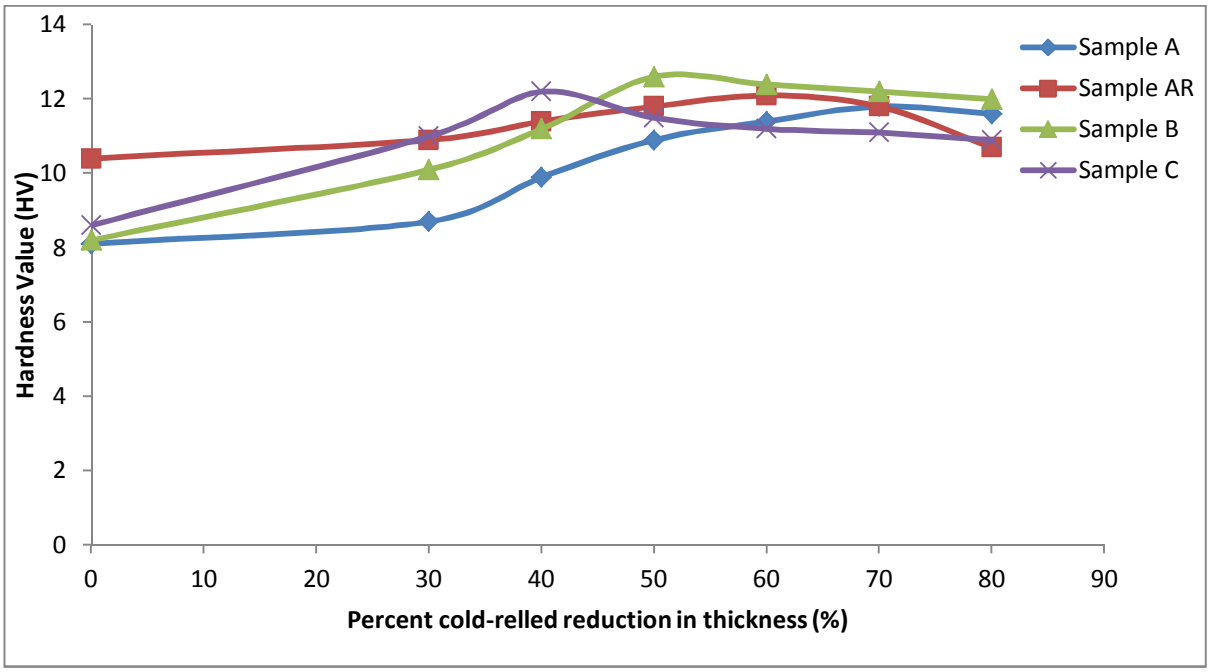


Figure 5.3: Graph of hardness values against cold-rolled reduction in thickness for the investigated alloy samples of AA 8011.

The microvicker hardness values plotted against percent cold-rolled reduction in thickness (Figure 5.3) of as-cast and as-received alloy samples increased steadily up to certain reductions in thickness. This could be attributed to strain hardening tendency of the alloy samples under investigation caused by cold rolling operation.

The hardness values of the investigated alloy samples A, AR, B and C increased progressively and reached peak levels at 70%, 60%, 50% and 40% reductions in thickness respectively. After the attainment of these peak levels of hardness property, all samples displayed decrease in hardness with increasing percent reduction in thickness. This observation is in agreement with Chang and Shan (2003) who reported that dislocation density in the interiors of the grain decrease with increase in strain leading to a situation in most interiors to become eventually free of dislocation after a large deformation resulting

to a reduced hardness value. Conclusively, the decrease in hardness of the alloys after large deformation is as a result of decrease in dislocation density in the interior of subgrains while the obtained lower hardness values with higher iron content can be linked to a high dislocation density originating from high iron intermetallic particles.

5.7 Effect of Iron Content on Impact Strength of Cold-rolled Samples of AA 8011

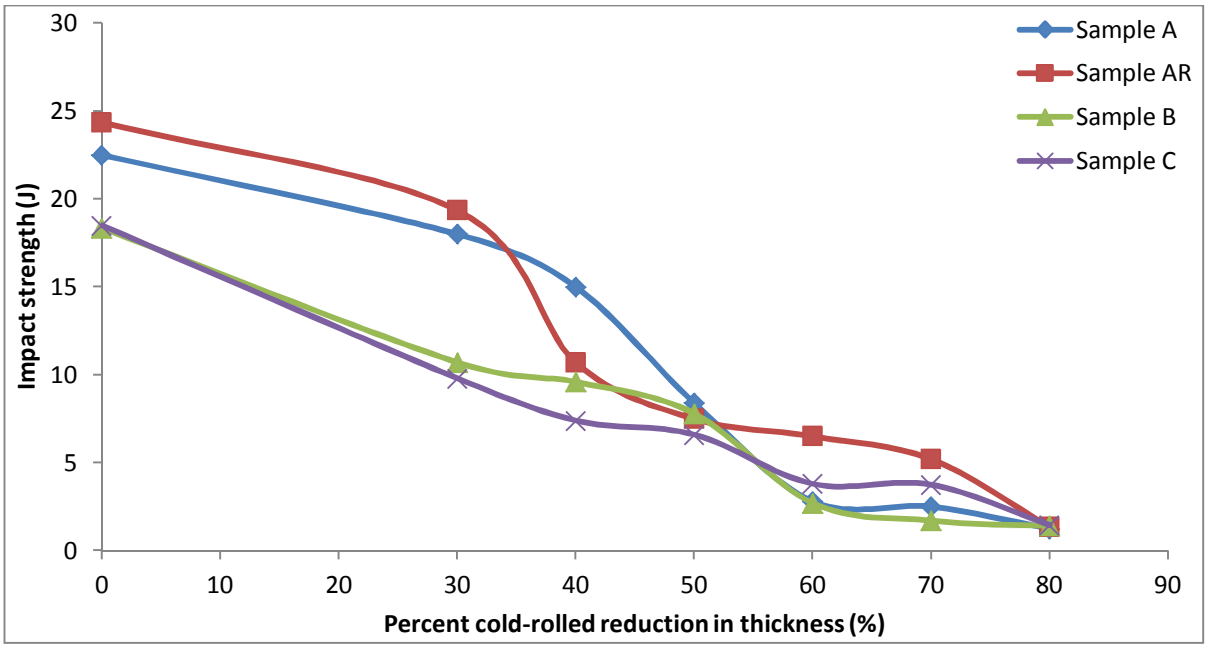


Figure 5.4: Graph of impact strength against cold-rolled percent reduction in thickness

The toughness values of the samples decreased progressively with increasing percent cold-rolled reduction in thickness with the sample AR displayed the highest impact property in as-received and at 30% reduction in thickness (Figure 5.4). This trend could be due to thermomechanical process (rapid solidification and hot rolling in a single operation) which accompanied the twin-roll casting method employed in the casting of the test samples as previously observed by Sanguinetti *et al.,* (2000). As highlighted, the specific thermal and mechanical treatments usually improve the mechanical properties of the alloy in general.

A corresponding increase in iron content led to a progressive decrease in toughness with increasing percent reduction in thickness at 40% and 50%. This could be due to high concentration of iron-rich intermetallic phase particles, suggesting a higher potential for fracture by the mechanism of coalescence when subjected to impact load and this is in agreement with the work of Salem, (2007).

From 60% reduction in thickness and above, the toughness values of the samples are almost equal but show a slight increase with increasing iron content. This little increment in toughness property might be attributed to the high level of intermetallic particles in alloys of higher iron contents which broken down into very fine dispersion particles by cold rolling operation giving rise to high grain boundaries structure thereby improving the impact strength.

5.8 Effect of Iron Content on Microstructures of Cold-rolled Samples of AA 8011

From the micrographs of as-received and as-cast samples shown in Plates C1, the aluminium matrix contained volume fractions of intermetallic phases predominately $FeAl_3$ and AlFeSi crystals. These crystals are finely dispersed within the matrix phase. As can be clearly observed in the as-cast samples, the crystals become larger in size and form interdendritic network as iron content in the alloy increases. In agreement with the finding of Sanders *et al.* (2004), the grains of as-received alloy cast by twin-roll casting method are finer than the other alloys because of the segregation of alloying elements in the as-cast condition at approximately the center of the strip thickness due to the shearing action of the rolls on the formed dendrites.

The ensuring squeezing of the interdendritic liquid towards the center enriched its concentration, giving rise to a region that contained higher amount of AlFeSi intermetallic phases. This observed phenomenon is a justification of the good mechanical properties obtained in the as-received samples.

The micrographs of cold-rolled samples shown in Plate C2 revealed a segregation of $FeAl_3$ and AlFeSi intermetallic phases in aluminium matrix. With an increase in percent reduction in thickness up to 80%, the fragmented grains become denser being elongated in the rolling direction. The redistribution of impurities that occurred during the rolling process resulted in segregation reduction observed in the samples at 80% reduction in thickness.

5.9 Evaluation of Lubricants in Cold Rolling Process

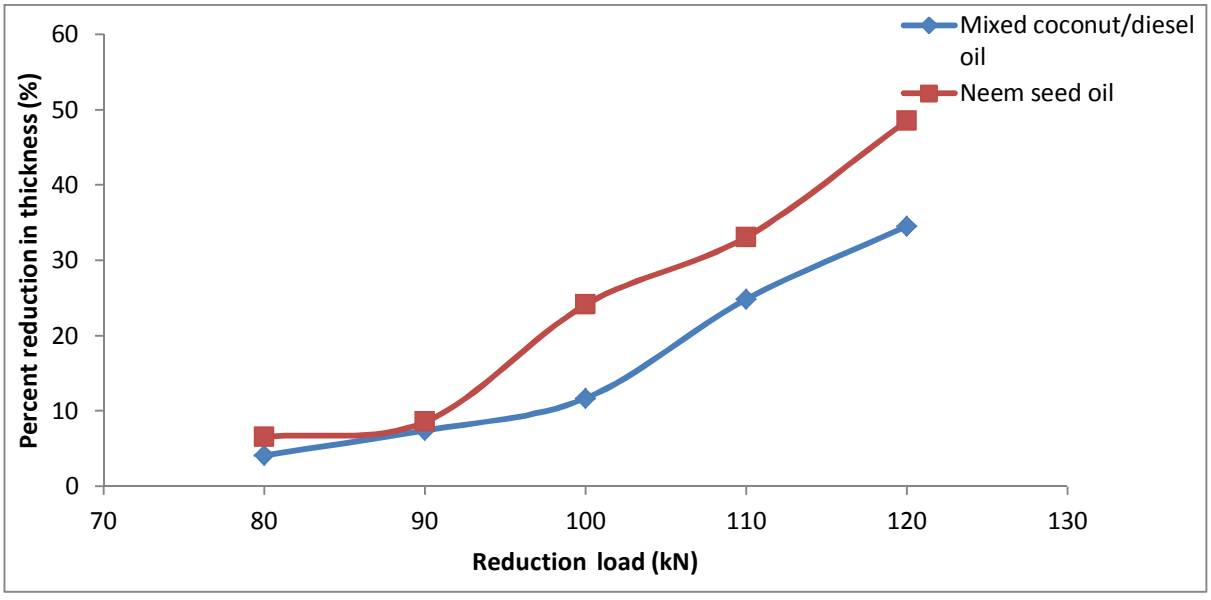


Figure 5.5: Reduction capacity of the investigated oils under plane strain compression test.

From the plot of percent reduction in thickness against reduction load (Figure 5.5), it was revealed that neem seed oil performed better than mixed coconut/diesel oil at any specific

load and the difference in performance was more pronounced at higher loads. The result of Gas Chromatography Mass Spectroscopy shown in Table 4.8 revealed the presence of oleic acid as the only fatty acid in mixed coconut/diesel oil whereas myristic, palmitic, stearic, oleic and linoleic acids were present in neem seed oil. In accordance with Babaagba (1986), the carboxylic groups of the fatty acids molecules oriented themselves with the metal surfaces which results in the formation of a film of fatty acid molecules on the metal surfaces. These film layers actually isolate the surface forces of the metal from the work rolls depending on the chain length of the fatty acid, and the friction is substantially reduced leading to higher deformation when neem seed oil was used as lubricant. Long straight hydrocarbons which are the major components of mixed coconut/diesel oil are saturated compounds which contain no polar (reactive) group to enhance friction reduction. This accounted for low values of deformation obtained when mixed coconut/diesel oil was used as lubricant.

The higher percentage of unsaturated fatty acids (oleic-49.46% and linoleic-16.77%) in neem seed oil compared to only oleic acid-1.38% in mixed coconut/diesel oil may also be the reason for high performance obtained under neem seed oil lubricant, as a result of their high affinity to react and adhere strongly to the workpiece and tools surfaces, causing long chain to be oriented approximately at right angles to the metal surface thereby minimizing metal-to-metal contact and hence friction is reduced.

Fatty acids tend to be more effective in friction reduction because of their ability to react with active oxide surface of the metal to form soap (Dave, 1995). The ease with which oil can form soap in mechanical working operation help in minimizing friction by the formation of adherent layer which separate the workpiece from the tool. These implies

that lubricity of any oil also depends on its saponification value which indicates the ease with which the oil form soap. Neem seed oil has 180.92 mg $KOHg^{-1}$ saponification value as compared to mixed coconut/diesel oil that has 25.25 mg $KOHg^{-1}$. This might also be the reason for low performance observed in mixed coconut/diesel oil when used as lubricant.

5.10 Evaluation of Proportions of Mixture of Coconut and Diesel Oils in Cold Rolling Process

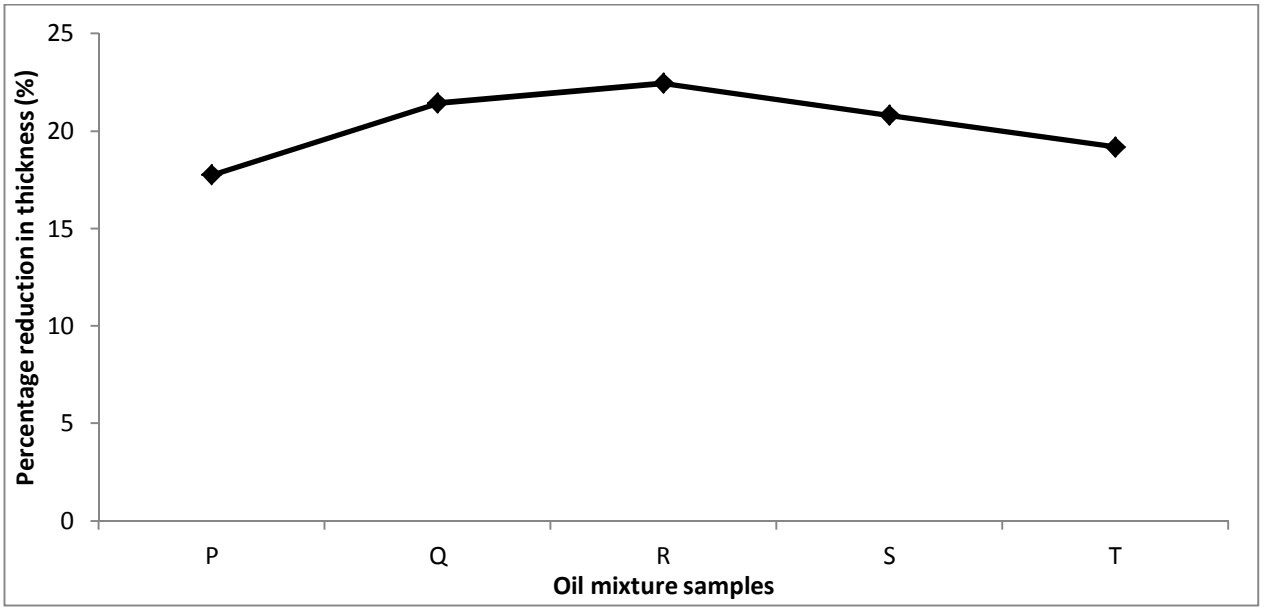


Figure 5.6: Reduction capacity of the locally sourced coconut oil mixed with diesel in various proportions under plane strain compression test.

The inability of Gas Chromatography Mass Spectroscopy to reveal the presence of all the fatty acids in mixed coconut/diesel oil (factory rolling oil) prompted further research on the optimum proportion of mixture of these oils that will enhance the highest friction reduction in cold rolling of the aluminium alloys. As shown in Figure 5.6, the mixture of the two oils in different proportions gives the highest percentage reduction in thickness at 70% diesel and 30% coconut oil at 100kN load.

According to Peter *et. al.* (2011), the formulations of straight oils lubricants contain no water and are comprised of petroleum and/or vegetable oils. Animal, marine, or vegetable oils may also be used singly or in combination with mineral oils to increase wetting action and lubricity (Peter *et. al.,* 2011). Therefore the increased in percentage reduction in thickness obtained with increased percentage of coconut oil in the mixture might be due to high level of wettability of the lubricant which improved its lubricity and the lubricant became warm at 70% diesel and 30% coconut oil given rise to high potential for friction reduction.

As more oil was being introduced in to the mixture, the reaction of the lubricant with the metal surface became lower due to the cooling action of the lubricant and this resulted to reduction in lubricity which accounted for gradual drops in percentage reduction in thickness observed in Figure 5.6.

CHAPTER SIX

6.0 SUMMARY, CONCLUSION AND RECOMENDATIONS

6.1 Summary

Commercial aluminium alloy 8011 has a wide range of applications owing to the fact that it can be deformed by mechanical working operation such as rolling. However, rolling process is known with some defects which usually affect the quality of the rolled products. In this research work, effort has been made to investigate edge cracking defect which usually accompanies rolling process from composition and lubrication points of view. Based on the results obtained, it was observed that up to a maximum iron content of 0.931%, AA 8011 could be cold-rolled to a maximum of 60% reduction in thickness without emergence of edge cracking defect. Below 0.9%Fe, AA 8011 could be successfully cold-rolled without experiencing edge cracking defect and above 0.9%Fe, the defect is unavoidable at higher reductions in thickness of 70% and 80%. Neem seed oil is more effective than mixed coconut/diesel oil as a means of edge cracking reduction due to its higher lubrication efficiency.

6.2 Conclusion

Based on the experimental finding, aluminium alloy 8011 generally exhibits softening characteristics as it was displayed by its maximum ultimate tensile strength of 176.45MPa at 60% reduction in thickness. On reaching the peak hardness values, all samples displayed decreasing in hardness property for a given levels of percent reductions in thickness- a behaviour which is in general agreement with the work of Xing *et al.* (2001). Due to its softening behaviour when subjected to mechanical working operations, AA

8011 generally exhibits excellent ductility. Samples of AA 8011 containing more than 0.9%Fe revealed higher tensile strength when cold-rolled to 80% reduction in thickness.

Performance evaluation of the lubricants (neem seed and mixed coconut/diesel oils) in plane strain compression test revealed that at any particular deformation and load reduction, neem seed oil performed better than mixed coconut/diesel oil as friction reduction in cold rolling of AA 8011. The mixture of local sourced coconut and diesel oils in different proportions gives the highest percentage reduction in thickness at 70% diesel and 30% coconut oil.

The difficulty of reducing edge cracking defect to an acceptable level experienced by Tower Aluminium Rolling Mills may be due to the following factors as can be deduced from experimental results:

- The iron composition of the alloy might have been above 0.9%Fe or exceeded the ranges of AA 8011 there by forming intermetallic particles that are so difficult to deform without encountering edge cracking at higher deformations.
- The low level of fatty acid present in the lubricant (mixed coconut/diesel oil) used as rolling mills oil.

6.3 Recommendations

Edge cracking defect greatly influence the quality of the rolled plate or strip of metal and its alloys. The possibility of reducing this defect to a tolerable level consists of investigating the parameters which contribute to the defect. Therefore the following recommendations were suggested for future work:

The reduction ratio per pass that will give the effective surface finish with acceptable level of edge cracking should be investigated. Defects such as wavy edge, zipper cracks in center of strip and alligatoring which are common defects in commercial rolling of alloys need further research work.

For Tower Aluminium Rolling Mills that is currently experiencing the edge cracking problem in its cold rolling operation of its aluminium products; scrap processing must be undertaken for adequate control of materials (most especially iron content) charges into melting furnace which may promote edge cracking defect in rolling process. Blends of local vegetable fatty acids oil could be considered as alternative lubricant in cold rolling operation of aluminium alloy 8011.

REFERENCES

Agwandas A. K. (1988). Evaluation of local oils for cold rolling of aluminium sheets. Unpubished B. Eng. Degree Project, Ahmadu Bello University, Zaria, Nigeria.

Akshay G. P. and Ibrahim M. (2008). Mechanical properties of Zn-9%Al-3%Cu alloy after equal channel angular extrusion. *Proceedings of the XIth International Congress and Exposition,* Society for Experimental Mechanics Inc. Orlando, Florida USA, pp 1-7.

Atkins A. G. (1974). Hydrodynamic lubrication in cold rolling. *International Journal of Mechanical Science,* Pergamon Press, Great Britain, 16, 1-19.

Babaagba R. S. (1986). Evaluation of local oils as lubricants in deep drawing operations. Unpublished M.Sc. Thesis, Ahmadu Bello University, Zaria Nigeria.

Boldetti C., Pinna C. and Howard C. (2006). Measurement and prediction in plane strain compression tests of AA 5182. *Journal of Material Science and Technology,* 22(11), 1380-1386.

Caceres C. H., Svensson I. L. and Taylor J. A. (2003). Strength-ductility of Al-Si-Cu-Mg casting alloys in T6 temper. *International Journal of Cast Metals Res.,* 15, 531-543.

Chang J. Y. and Shan A. (2003). Microstructure and mechanical properties of AlMgSi alloys after equal channel angular pressing at room temperature. *Materials Science and Engineering Journal,* A327, 165-170.

Dave P. (1995). Industrial lubrications cleaning and waste minimization. *Precision Cleaning Preceeding,* pp 208-216.

Dieter G. E. (1988). *Mechanical metallurgy.* SI Metric Edition, McGraw-Hill Book Company, London, pp 587.

Fabia G., Giulio T., Franco B. and Roberto M. (2009). Correlation between microstructure and mechanical properties of Al-Si die cast engine blocks. *Material Science and Technology Journal,* 27, 1-10.

Fang X., Shao G., Liu Y. Q. and Fan Z. (2011). Effects of intensive forced melt convection on the mechanical properties of Fe-containing Al-Si based alloys. *Brunel Centre for Advanced Solidification Technology (BCAST),* Brunel University, Uxbridge, Middlesex, UB8 3PH, UK, pp 1-11.

Gaminana J. O. (2011). Evaluation of neem (*azadirachta indica*), tiger nut (*cyperus esculentus*) and false walnut (*canarium schweinfurthii*) oils as metalworking lubricants. Unpublished M.Sc. Degree Thesis, Ahmadu Bello University, Zaria, Nigeria.

Ghosh S., Li M. and Gardiner D. (2004). A computational and experimental study of cold rolling of aluminium alloys with edge cracking. *Journal of manufacturing Science and Engineering,* 74-82.

Haga T., Sakaguchi H., Watari H. and Kumai S. (2008). High speed twin roll casting of 6061 alloy strip. *Archives of Materials Science and Engineering Journal,* 31, 49-52.

Haiba X. (2011). The research on the edge crack of cold rolled thin strip. Unpublished Ph. D Thesis, School of Mechanical, Materials and Mechatronic Engineering, University of Wollongong.

Hosford W. E. (1966). Plane strain compression test of aluminium crystals. *Acta Metallurgica*, 14, pp 1084-1094.

Ikuo Y., Takashi N. and Tsuyoshi H. (2005). Stress strain behaviour of magnesium alloy A231 in plane strain compression. *JSME International Journal,* 18(4), 299-304.

John A. S. (1991). *Metal deformation processes/friction and lubrication*. Marcel Dekker Inc., New York, pp 242.

John A. T. (2009). The effect of iron in Al-Si casting alloy. *Cooperative Research Centre for Cast Metals Manufacturing (CAST),* The University of Queensland, Brisbane, Australia, pp 1-10.

Kuijpers N. C. W., Kool W. H., Koenis P. T. G., Nilsen K. E., Todd I. and Van der Zwaag S. (2003). Assessment of different techniques for quantification of α-Al(FeMn)Si and β-AlFeSi intermetallics in AA 6xxx alloys. *Materials Characterization,* 49, pp 409-420.

Lu L. and Dahel A. K. (2005). Iron-rich intermetallic phases and their role in casting defect formation in hypoeutectic Al-Si alloys. *Metallurgical and Materials Transactions,* 36A, pp 819-835.

Lugt P. M., Wemekamp A. W. and Napel W. E. (1993). Lubrication in cold rolling; elato-plasto-hydrodynamic lubrication of smooth surface. *Hoogovens Research Laboratory*, University of Twente, Enschede, Netherland, pp 203-214.

Mbuya T. O., Odera B. O. and Nganga S. P. (2003). Influence of iron on castability and properties of aluminium silicon alloys. *International Journal of Cast Metals Research,* 16(5), 45-465.

Na D. H. and Lee Y. (2008). FE simulation of edge crack initiation and propagation of conventional grain orientation electrical steel. *International Journal of Modern Physics B,* 22(31&32), 5465-5470.

Naser A. and Tom Y. (2008). Rolling laboratory lecture note in conjunction with fundamentals of modern manufacturing engineering. *Industrial & System Engineering and Welding Engineering,* Ohio State University, USA, pp 21.

Oginsky Y. K. (2011). The force pattern in the deformation zone at steady rolling process. *Journal of Metallurgical and Mining Industry,* National Metallurgical Academy, Ukraine, 3(1), pp 10-4.

Oyinlola A. K. (1976). Strain distribution analysis in ring upset forging and hot-rolling by photoplasticity. Unpublished Ph.D Thesis, Iowa State University, Ames Iowa, United State of America.

Peter B., Shiv G. K. and Richard E. D. (2011). Transiently stable emulsions for metalworking fluids, *Illinois Sustainable Technology Center Prairie Research Institute,* University of Illinois at Urbana-Champaign, pp 8.

Rowe G. W. (1968). *An introduction to the principles of metalworking*. Edward Arnold Ltd, London, pp 26.

Salem S. (2007). The influence of iron on the microstructure and mechanical properties of cast Al-Si alloys. Unpublished Ph.D Thesis, Jonkoping University, The School of Engineering Component Technology, Sweden.

Sanders R. E., Hollinshead P. A. and Simielli (2004). Industrial development of non-heat treatable aluminium alloy. *Materials Forum,* Institute of Materials Engineering, Austral/Asia, 28, pp 53-64.

Sanguinetti F., Riberio F. G. and Rocha L. (2000). Study of development in AA 8023; kinetics and morphological aspect. *Scripta Mater,* 43, pp 929-934.

Sansome D. H. (1975). Factors affecting the shape of strip emerging from a rolling mill. *Metal Technology,* pp 522-530.

Schey J. A. (1966). Prevention of edge cracking in rolling by means of edge restraint. *Journal of the Institute of Metals,* 193-198.

Seifeddine S. and Svensson I. L. (2009). The influence of Fe and Mn content and cooling rate on the microstructure and mechanical properties of A380-die casting alloys. *Metallurgical Science and Technology Journal,* 27, 1-20.

Shabestari S. G., Mohammed M., Emamy M. and Campbell J. (2002). Effect of Mn and Sr on intermetallics in Fe-rich eutectic Al-Si alloys. *International Journal of cast Metal Research,* 15(1), 17-24.

Siddiqui R. A., Abdullah H. B. and Al-Belushi K. R., (2000). Influence of aging parameters on the mechanical properties of 6063 aluminium alloy. *Journal of Materials Processing Technology,* 102, 234-240.

Sutcliffe M. P. F., Combarien R., Repoux M. and Montmitonnet P. (2002). Tribology of plane strain compression tests on aluminium strip using Tof-Sims analysis of transfer films. *Journal of Wear*, 254, 65-79.

Tajally M., Huda Z. and Masjuki H. H. (2009). Effect of cold rolling on bending and tensile behaviour of 7075 aluminum alloy. *Journal of Applied Sciences,* 9, 3888-3893.

Tang S. K. and Sritharan T. (1998). Morphology of β-Al_5FeSi intermetallic in Al-7Si alloy casting. *Material Science and Technology,* 14, pp 738-742.

Taylor J. A., Schaffer G. B. and John D. H. (1999). The role of iron in the formation of porosity in Al-Si-Cu-based casting alloys. *Metallurgical and Materials Transactions,* 30 A (6), pp 1651-1655 (part 2).

Taylor J. A., John D. H., Barresi J. and Couper M. J. (2000). An empirical analysis of trends in mechanical properties of T6 heat treated Al-Si-Mg casting alloys. *International Journal of Cast Metal Research,* 12, 419-430.

Ullrich Aluminium Company Technical Data on Chemical Composition of aluminium alloys, code 6061 – 8011 (2008). Retrieved from http://www.ullrich.co.nz

Valiev R. Z. (2003). Recent developments of SPD processing for fabrication of bulk nanostructured materials. *Materials Science Forum,* 426-432, pp 237-244.

Varuzan K., Auton S., Mirko D. and Edvard S. (2005). Microstructure and formability development in Al strip casting for thin gauge foil production. *Association of Metallurgical Engineers Serbia and Montenegro Scientific paper,* pp 125-128.

Watts A. B. and Ford H. (1952). An experimental investigation of the yielding of strip between smooth dies. *Processing Institute of Mechanical Engineering,* B1, pp 448-453.

William D. C. (2009). *Material science and engineering*. John Wiley and Sons, New Delhi, India, pp 361

Xing Z. P., Kang S. B. and Kim H. W. (2001). Softening behavior of 8011 alloy produced by accumulative roll bonding process. *Scripta Material* 45, ActaMateria Inc. Published by Elsevier Science Ltd, pp 597-604.

Zainul H. (2009). Effect of degree of cold working and recrystallization on the microstructure and hardness of commercial purity aluminium. *European Journal of Scientific Research,* 26(4), 549-557.

Zhang H. (2007). Effect of iron on the microstructure and mechanical properties of Al-Si alloys. *The Minerals, Metals and Materials Society,* Shanghai, China, pp 775-780.

APPENDICES

Appendix A

Plate A1 – A6: Edge cracking characteristics of aluminium alloy 8011 of varying degree of iron content cold-rolled to various reductions in thickness. Samples A- 0.708%Fe, AR- 0.857%Fe, B- 0.909%Fe, and C- 0.931%Fe (Samples A, B and C are as-cast alloys while sample AR is as-received alloy).



Plate A1: Aluminium Alloy 8011 cold-rolled to 30% reduction in thickness.

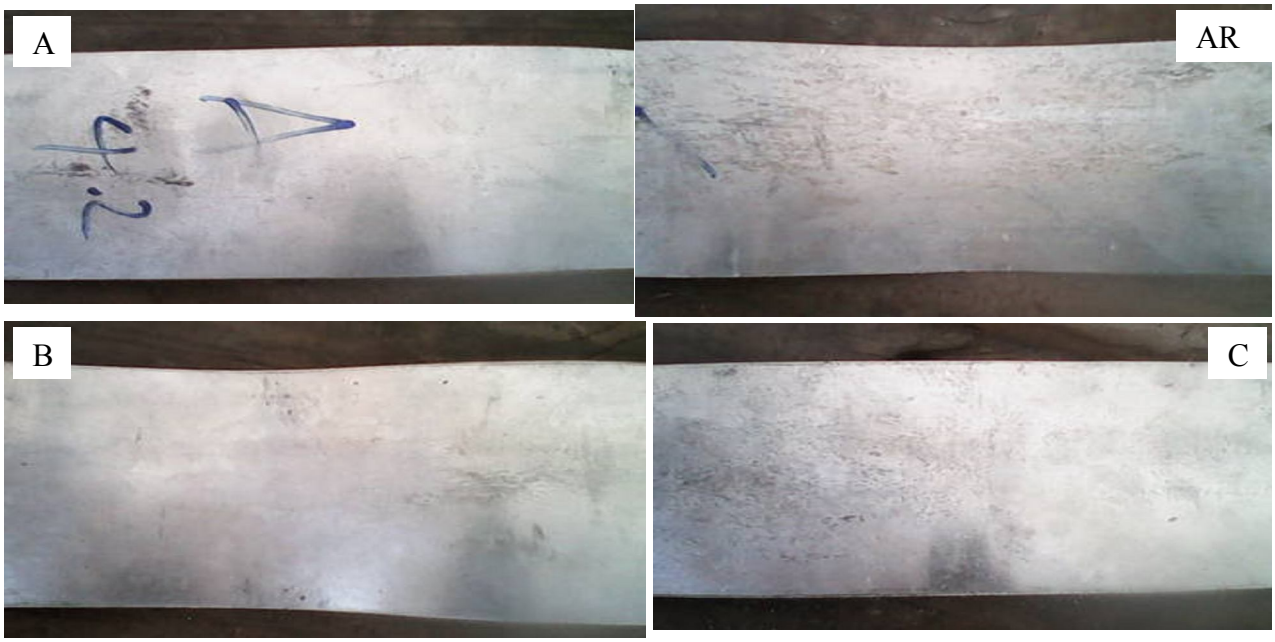


Plate A2: Aluminium Alloy 8011 cold-rolled to 40% reduction in thickness



Plate A3: Aluminium Alloy 8011 cold-rolled to 50% reduction in thickness



Plate A4: Aluminium Alloy 8011 cold-rolled to 60% reduction in thickness

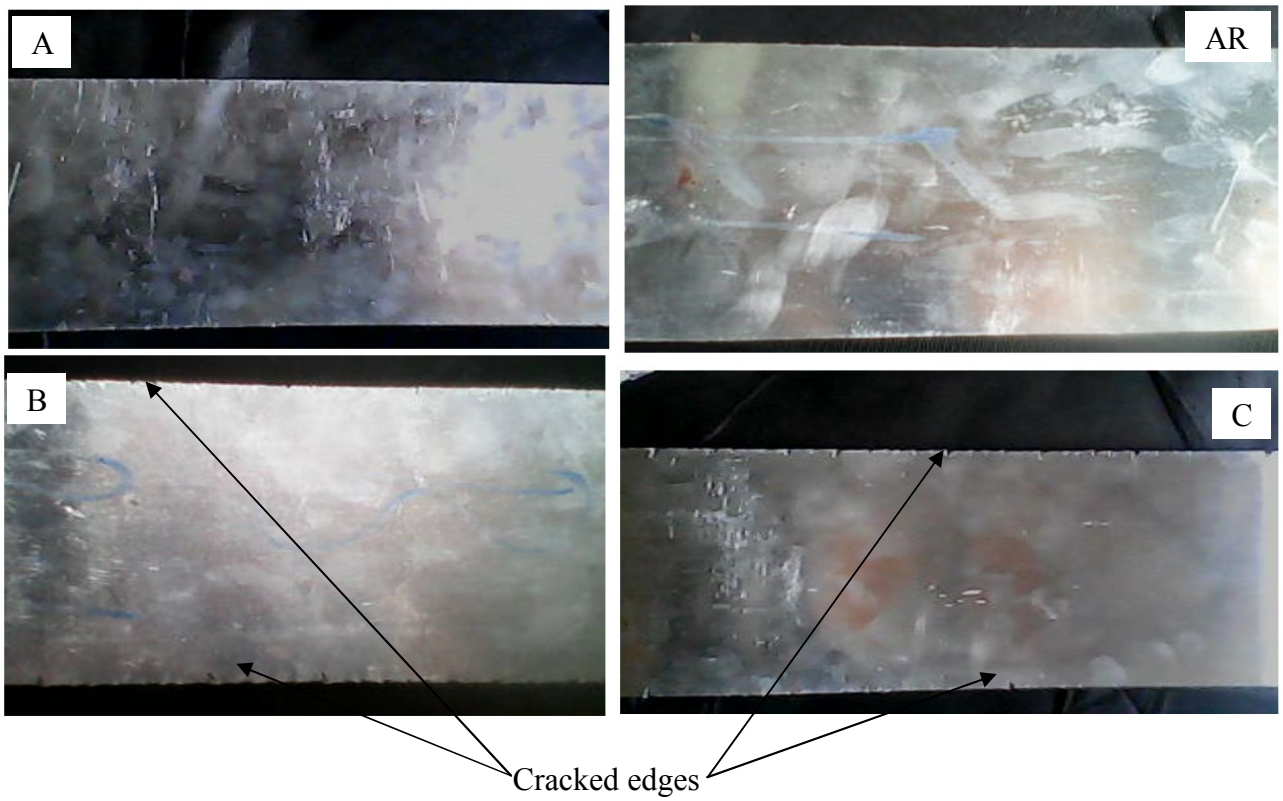


Plate A5: Aluminium Alloy 8011 cold-rolled to 70% reduction in thickness

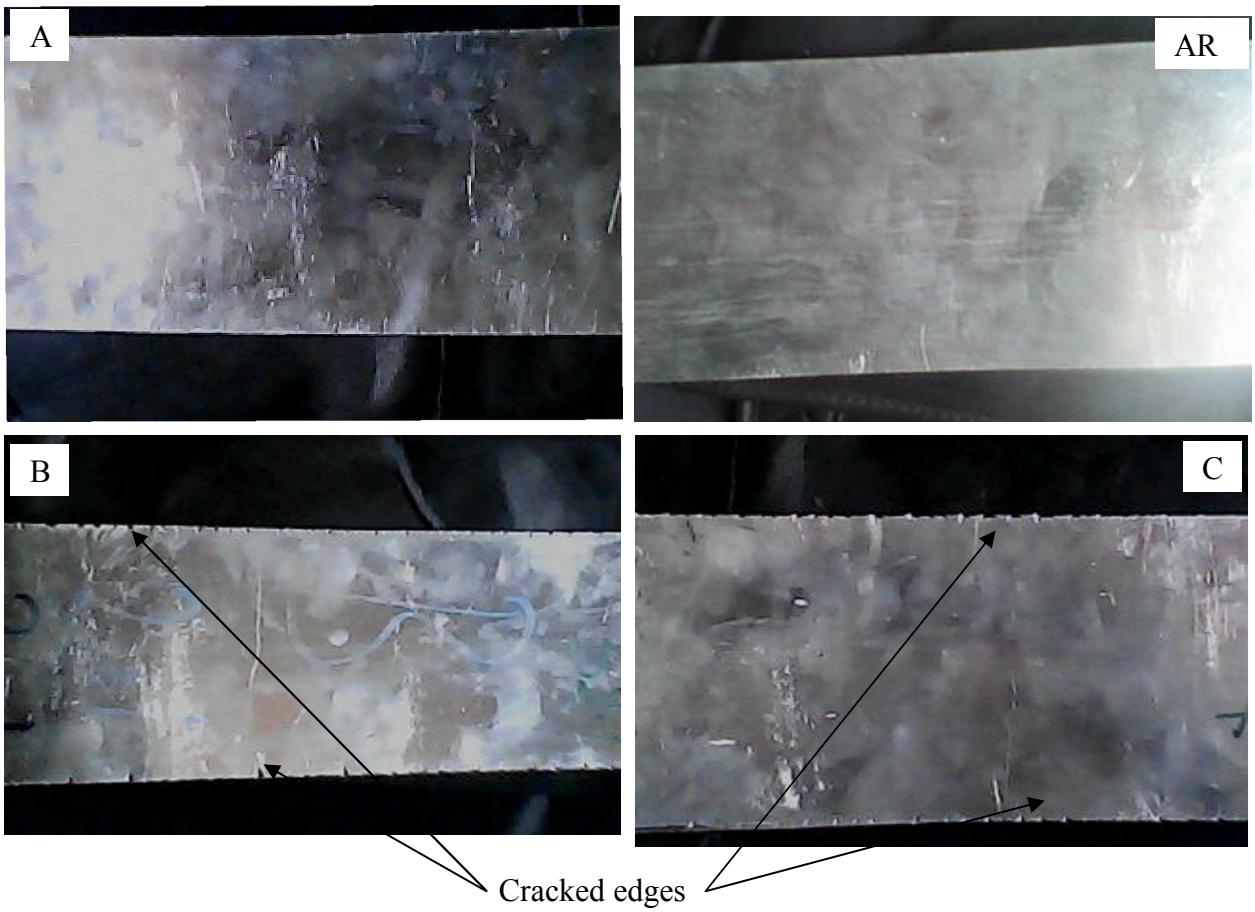


Plate A6: Aluminium Alloy 8011 cold-rolled to 80% reduction in thickness

Appendix B

Figures B1- B7: Stress-strain curves of as-received and as-cast samples of AA 8011 of varying iron contents cold-rolled to various reductions in thickness.

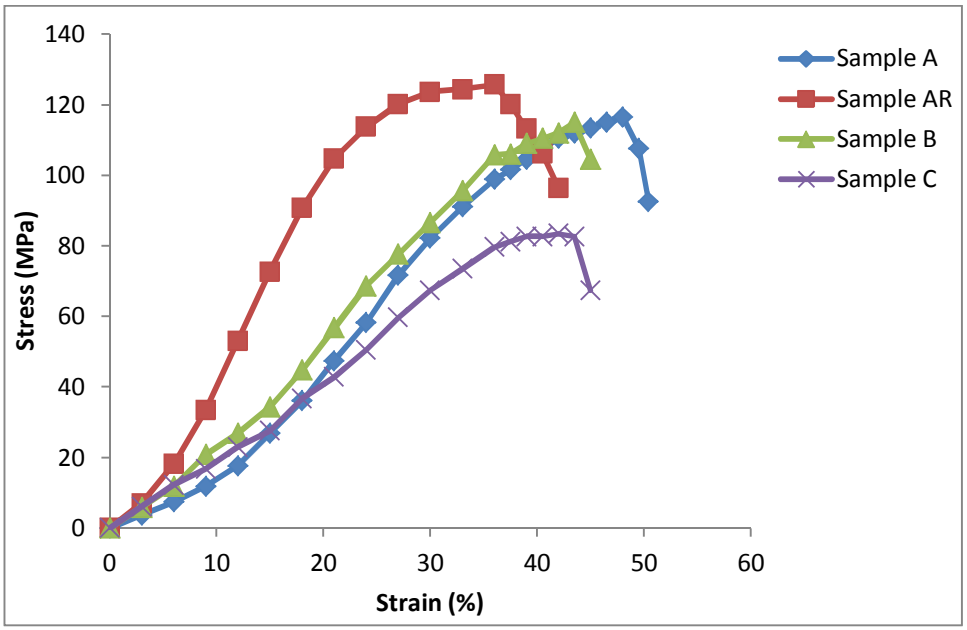


Figure B1: Stress-strain curves of as-cast and as- received samples

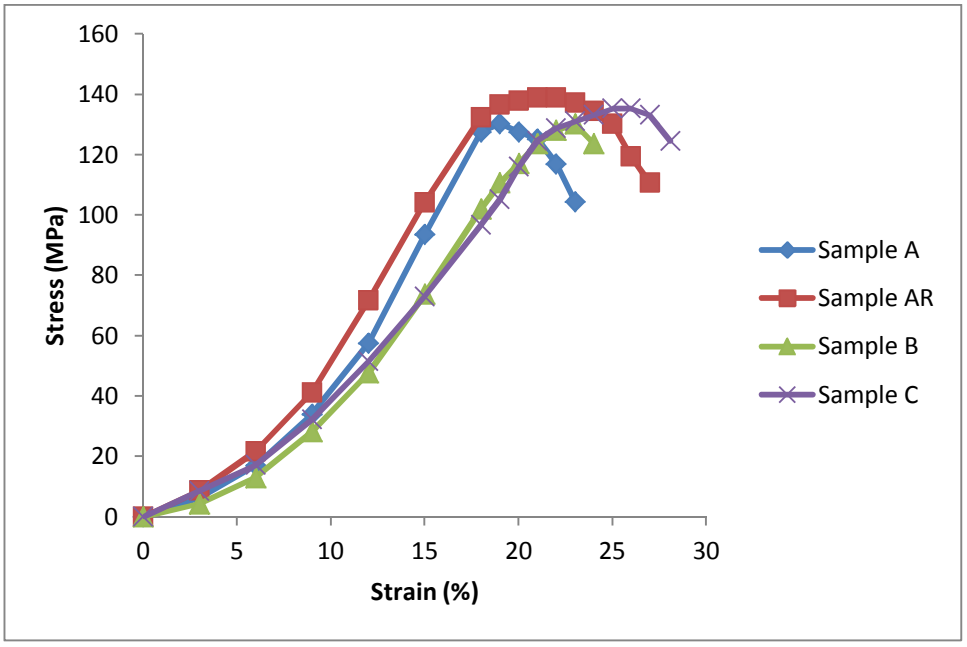


Figure B2: Stress-strain curves of samples cold-rolled to 30% reduction in thickness

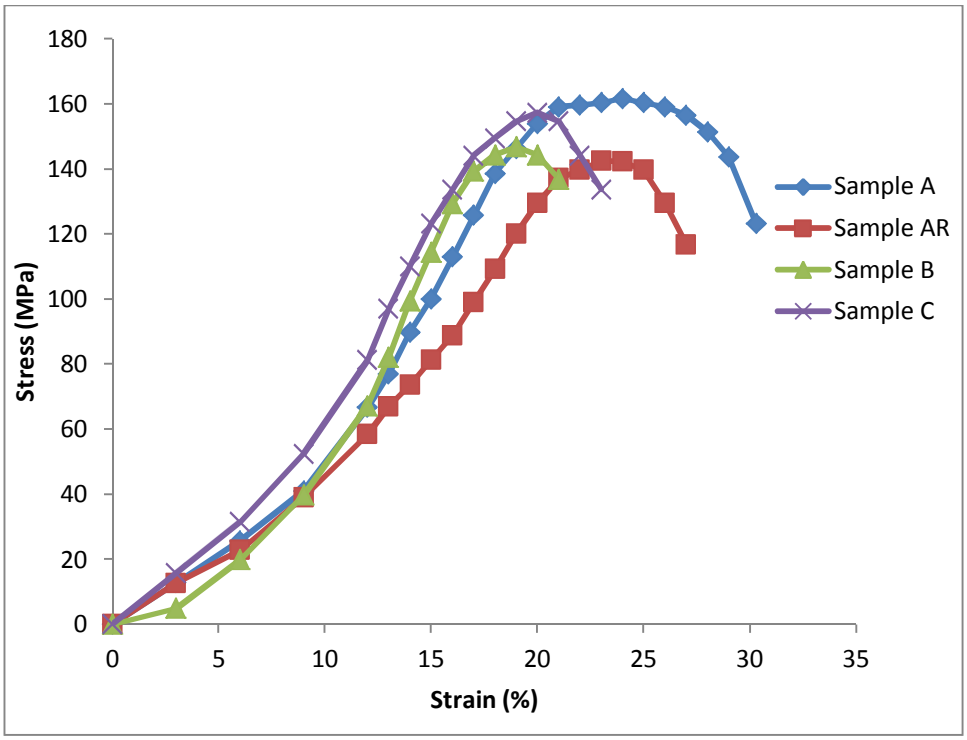


Figure B3: Stress-strain curves of samples cold-rolled to 40% reduction in thickness

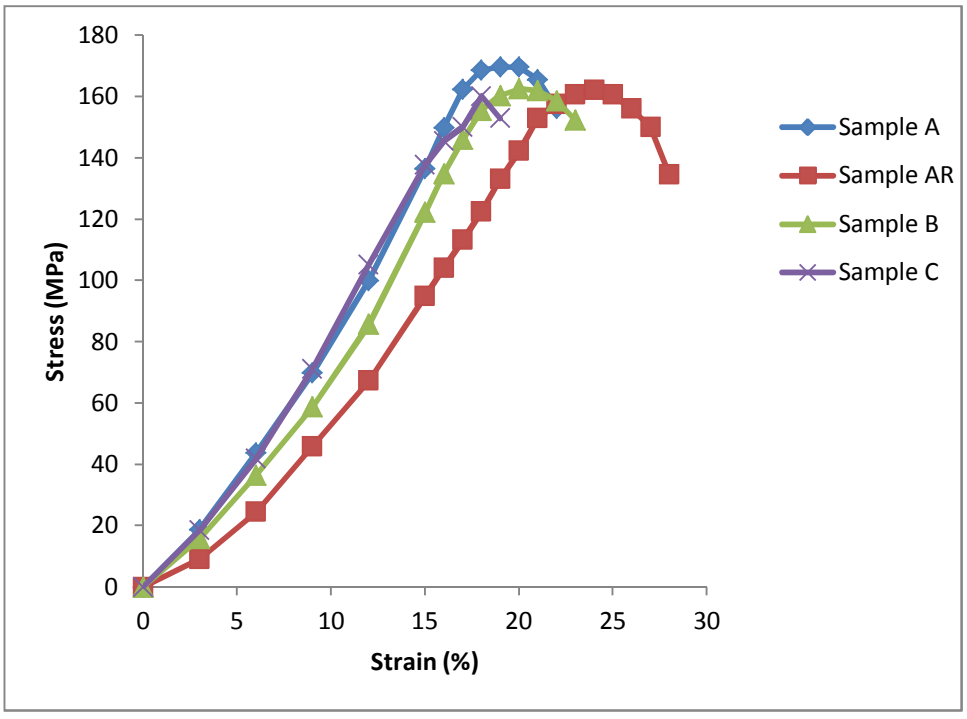


Figure B4: Stress-strain curves of samples cold-rolled to 50% reduction in thickness

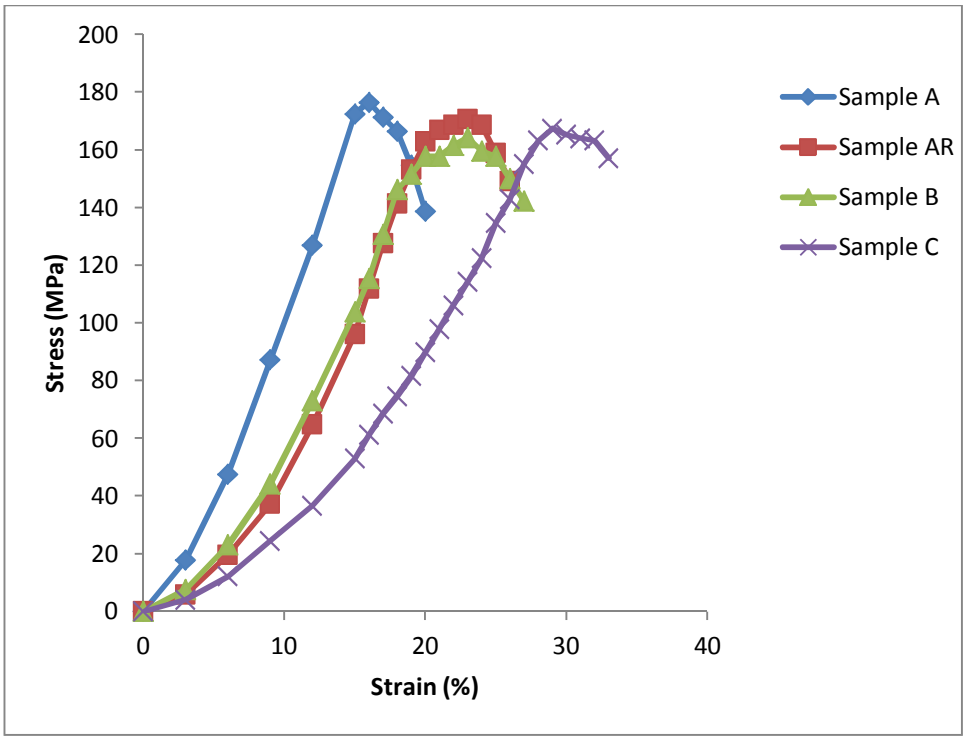


Figure B5: Stress-strain curves of samples cold-rolled to 60% reduction in thickness

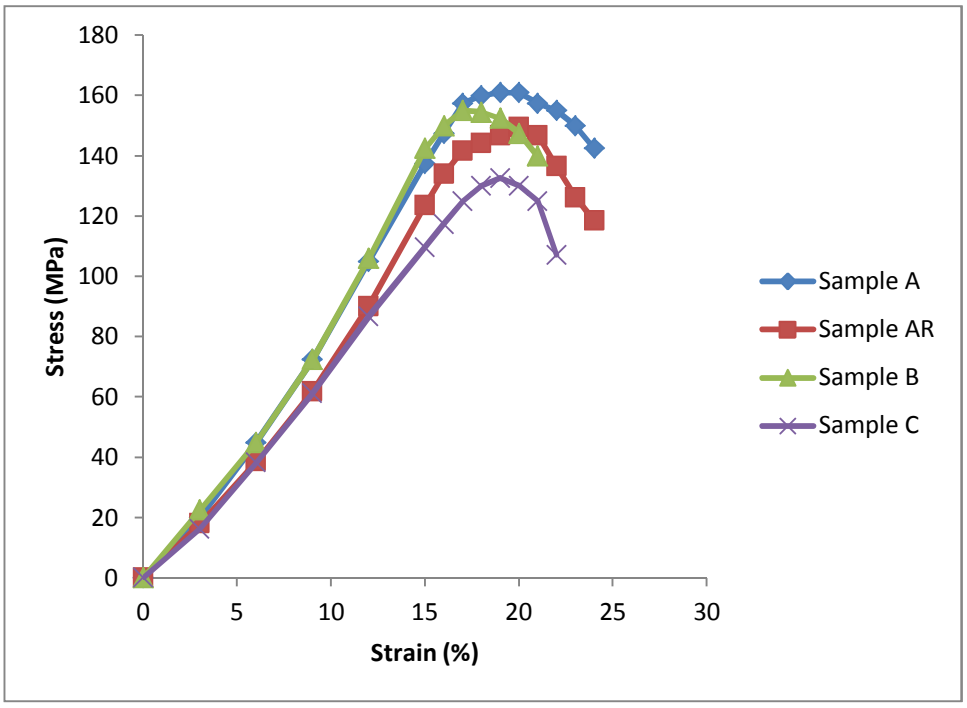


Figure B6: Stress-strain curves of samples cold-rolled to 70% reduction in thickness

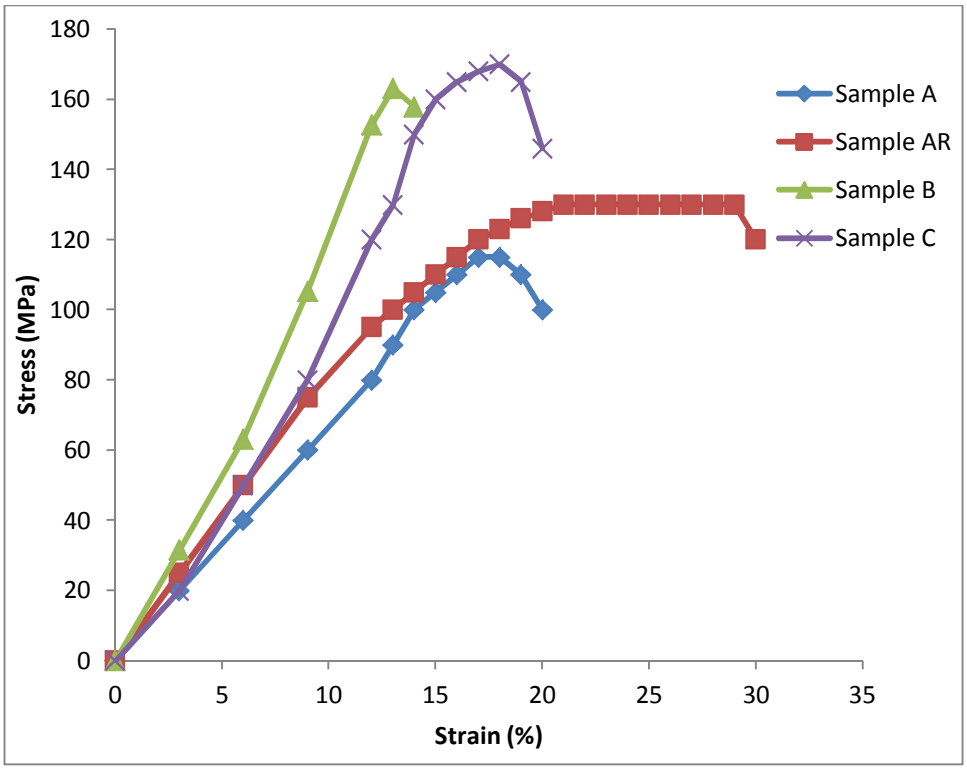


Figure B7: Stress strain-curves of samples cold-rolled to 80% reduction in thickness

Appendix C

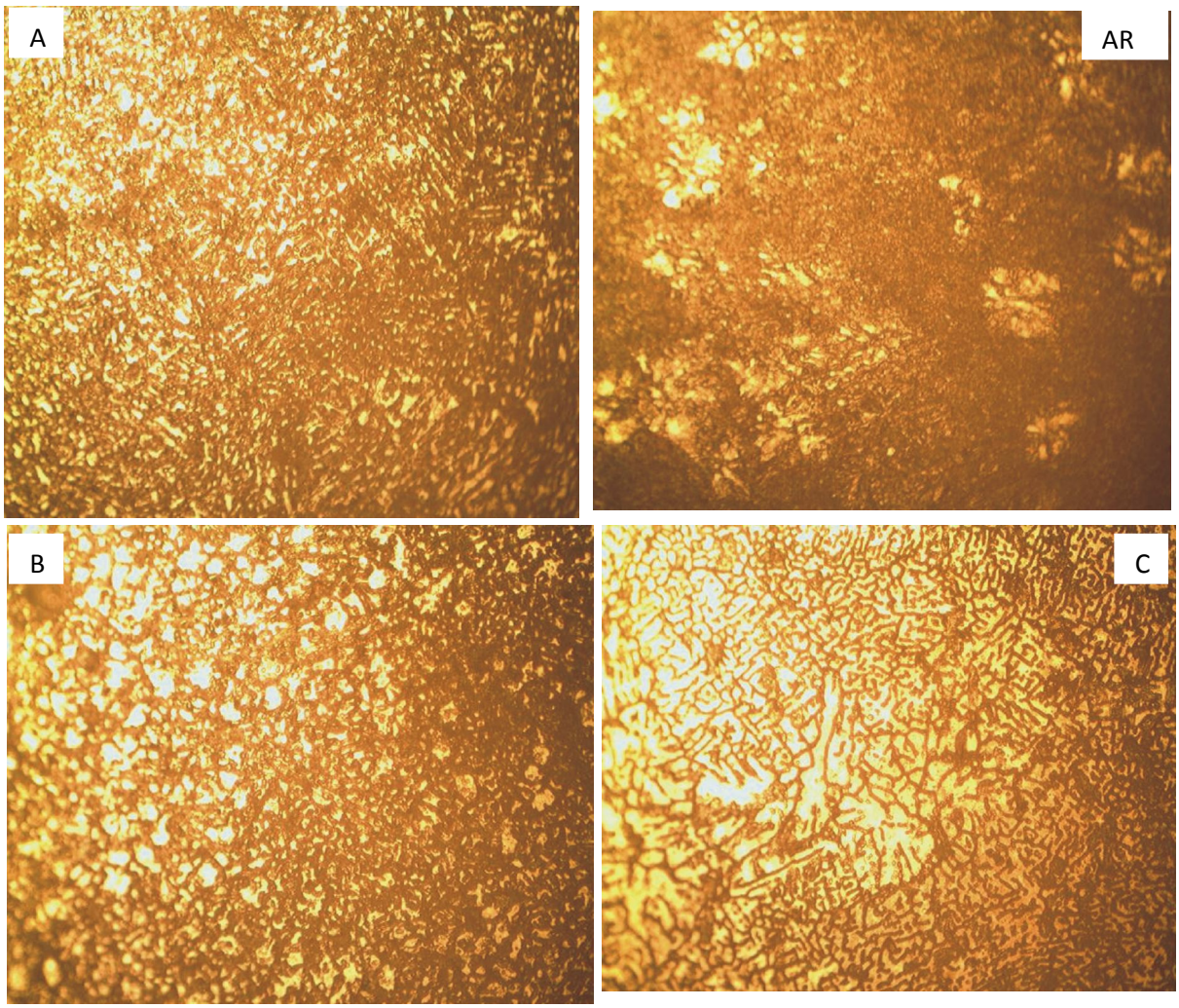


Plate C1: Optical micrographs of as-received and as-cast samples of AA 8011 of various levels of iron content; samples A- 0.708%Fe, AR- 0.857%Fe, B- 0.909%Fe, and C- 0.931%Fe. White spots are interdendritic of intermetallic particles distributed in aluminium matrix (yellow back-ground). X100.

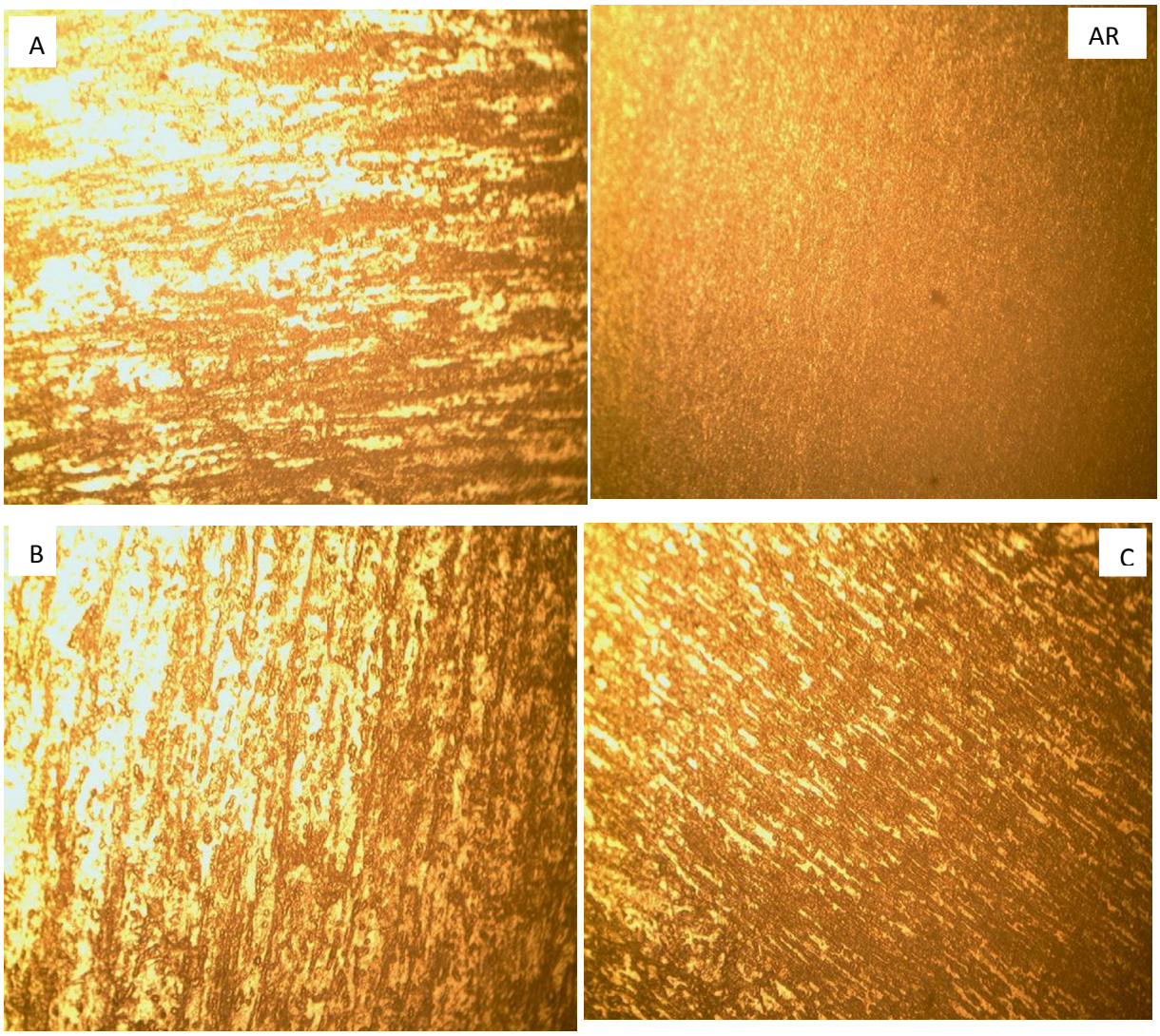


Plate C2: Optical micrographs of samples AA 8011 cold-rolled to 80% reduction in thickness. White spots are fragmentation of interdendritic particles elongated along rolling direction in aluminium matrix (yellow back-ground). X100.